MATERIALS
CHEMISTRY
FRONTIERS

Themed issue: In celebration of Prof. Fred Wudl's 80th Birthday

REVIEW

Check for updates

Two-dimensional halide perovskites featuring semiconducting organic building blocks

Yao Gao, [ID] [a] Zitang Wei,[a] Sheng-Ning Hsu, [ID] [a] Bryan W. Boudouris [ID] [ab] and Letian Dou [ID] *[ac]

Two-dimensional (2D) organic–inorganic hybrid halide perovskites exhibit unique properties, such as long charge carrier lifetimes, high photoluminescence quantum efficiencies, and great tolerance to defects. Over the last several decades tremendous progress has occurred in the development of 2D layered halide perovskite semiconductor materials and devices. Chemical functionalization of 2D halide perovskites is an effective approach for tuning their electronic properties. A large amount of effort has been made in compositional engineering of the cations and anions in the perovskite lattice. However, few efforts have incorporated rationally designed semiconducting organic moieties into these systems to alter the overall chemical and optoelectronic properties of 2D perovskites. In fact, incorporation of large conjugated organic groups in the spatially confined inorganic perovskite matrix was found to be challenging, and this synthetic challenge hinders a deeper understanding of the materials' structure–property relationships. Recently, exciting progress has been made regarding the molecular design, optical characterization, and device fabrication of novel 2D halide perovskite materials that incorporate functional organic semiconducting building blocks. In this article, we provide a timely review regarding this recent progress. Moreover, we discuss successes and current challenges regarding the synthesis, characterization, and device applications of such hybrid materials and provide a perspective on the true future promise of these advanced nanomaterials.

[a] *Davidson School of Chemical Engineering, Purdue University, West Lafayette, IN 47907, USA. E-mail: dou10@purdue.edu*
[b] *Department of Chemistry, Purdue University, West Lafayette, IN 47907, USA*
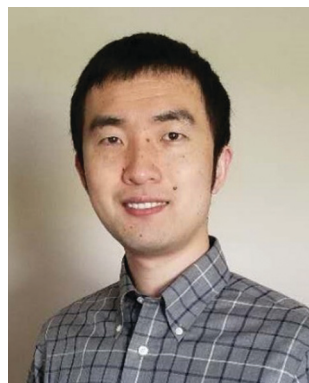[c] *Birck Nanotechnology Center, Purdue University, West Lafayette, IN 47907, USA*

1. Introduction to 2D halide perovskites

Halide perovskites [*i.e.*, materials with a chemical structure of ABX_3 (A = organic ammonium cation, Cs^+; B = Pb^{2+};

Dr Yao Gao is currently a postdoc research associate in the Davidson School of Chemical Engineering, Purdue University. He received his BS in Chemistry from Nanjing University in 2011. Then he joined Prof. Yanhou Geng's group at Changchun Institute of Applied Chemistry, Chinese Academy of Sciences, and obtained his PhD degree in Polymer Chemistry and Physics in 2017. Dr Yao Gao is now working on organic–inorganic hybrid two-dimensional halide perovskites in Prof. Letian Dou's group, his research interests include the synthesis and characterization of organic and hybrid semiconducting materials, and their applications in optoelectronics.
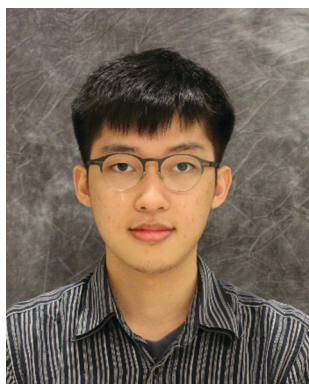
Yao Gao

Zitang Wei is currently a PhD student in the Davidson School of Chemical Engineering, Purdue University. He obtained his BS in Chemistry from UCSB in 2018. From 2016 to 2017, he was an undergraduate research fellow in Prof. Fred Wudl's group, focusing on design and synthesis of non-fullerene acceptors for organic photovoltaics. He joined Prof. Letian Dou's group as a graduate research assistant in 2018. His research interests include design and synthesis of novel conjugated organic ligands for two-dimensional organic inorganic hybrid perovskite materials.

Zitang Wei

X = Cl⁻, Br⁻, I⁻)] have emerged as a new class of solution-processed semiconductor materials with excellent optical and electronic properties.[1] As a subclass of halide perovskites, two-dimensional (2D) halide perovskites can be thought of as slabs cut from the three-dimensional (3D) ABX_3 parent structures (Fig. 1a), and these slabs can be obtained by cutting along the $\langle 100 \rangle$, $\langle 110 \rangle$, and $\langle 111 \rangle$ crystallographic planes of the parent 3D perovskite structure. In turn, this leads to three 2D perovskite families with different orientations. The $\langle 100 \rangle$-oriented perovskites are the subgroup of the perovskite derivative family with the richest amount of literature currently.[1–6] Based on the choice of the capping cation and relative position between the inorganic layers, this class of materials can be further divided into three types that are the: Aurivillius phase, Dion–Jacobson phase, and Ruddlesden–Popper (RP) phase. The RP phase that consists of 2D perovskite slabs interleaved with cations is most commonly observed in halide perovskites.[7,8] Specifically, the RP phase has the general chemical formula of $L_2A_{n-1}B_nX_{3n+1}$, where L is a large cation, A is a small cation [e.g., cesium and methylammonium (MA^+)], B is a divalent metal cation (e.g., Pb^{2+} and Sn^{2+}), and X is a halide. The variable n indicates the number of the metal halide octahedral layers between the two L cation layers. When n is infinite, the structure becomes a 3D perovskite. When $n = 1, 2, 3$, and up to a finite number, the structure constitutes an ideal quantum well with only a few atomic layers of BX_4^{2-} separated by L cations. The exact value of n can be relatively large, but increasing the value of n tends to becoming more challenging with respect to obtaining highly-crystalline materials. In these systems many of the repeating units can stack together through van der Waals forces to form bulk crystals. Notably, the n number can be specified by carefully controlling the chemical stoichiometry of the precursors in the solution. Currently, single crystals of n up to 7 have been obtained.[9] This structural diversity allows fine-tuning of their optical and electronic properties for a wide range of applications.

In addition to their tunable structures and properties, 2D halide perovskites are generally more stable against moisture than their 3D counterparts due to the hydrophobic nature of the organic spacer, making them promising for commercial applications. Specifically, the enhanced stability over the 3D parent structure has been attributed to the increased hydrophobicity from the organic layer formed by the L cations. Electronically, these 2D halide perovskites can be regarded as self-assembled multiple-quantum-well structures, in which the

Sheng-Ning Hsu

Sheng-Ning Hsu is currently a PhD student in the Davidson School of Chemical Engineering, Purdue University. He received his BS in Chemical Engineering from National Taiwan University in 2016. He then served as a research assistant in Prof. Wen-Chang Chen's group at the department of Chemical Engineering, National Taiwan University from 2017 to 2018. He started pursuing his PhD degree and joined Prof. Bryan Boudouris and Prof. Letian Dou's groups in 2018. His current research focuses on synthesizing organic–inorganic hybrid two-dimensional hybrid perovskites and their applications in optoelectronics.
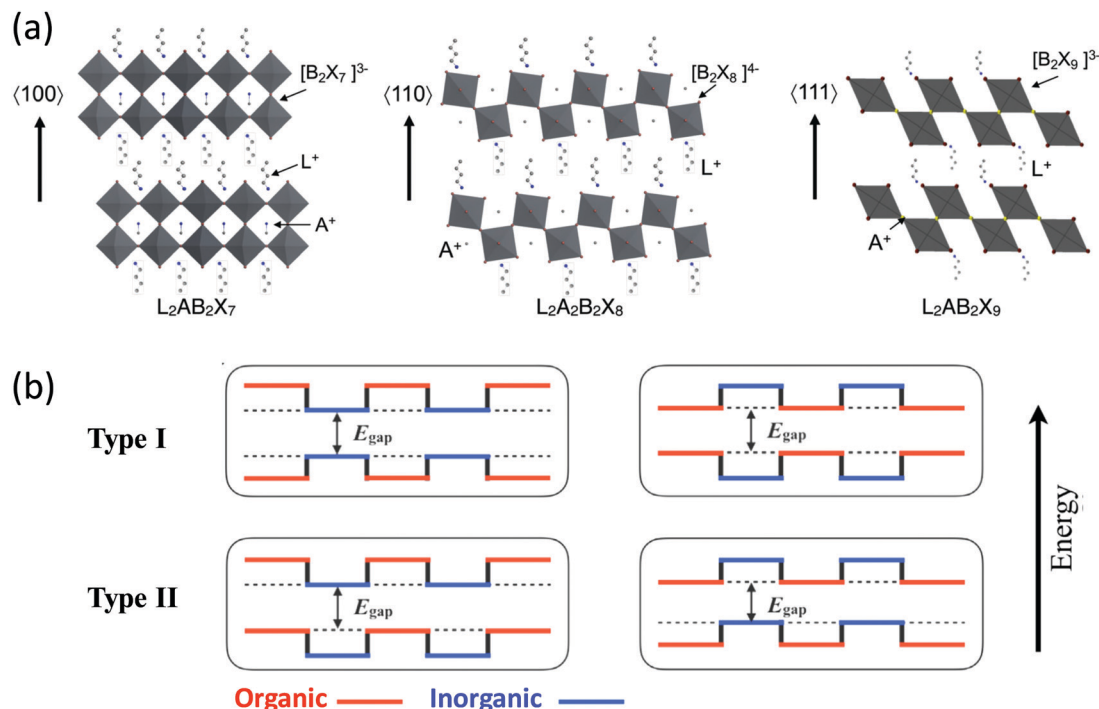
Bryan W. Boudouris

Bryan W. Boudouris is the Robert and Sally Weist Associate Professor in the Davidson School of Chemical Engineering and an associate professor (by courtesy) in the Department of Chemistry at Purdue University. He received his BS in Chemical Engineering from the University of Illinois at Urbana-Champaign. After receiving his PhD in Chemical Engineering from the University of Minnesota, he conducted postdoctoral research at the University of California, Berkeley. His team's work has been recognized with the AFOSR YIP Award, the DARPA YFA, the NSF CAREER Award, the AIChE Owens Corning Early Career Award, and the Saville Lectureship at Princeton University.

Letian Dou

Prof. Letian Dou joined the Davidson School of Chemical Engineering of Purdue University in 2017. He obtained BS in Chemistry from Peking University in 2009 and PhD in Materials Science and Engineering from UCLA in 2014. He discovered visible-light triggered topochemical polymerization with Prof. Fred Wudl at USCB in 2013. From 2014 to 2017, he was a post-doctoral fellow at the Department of Chemistry, UC-Berkeley and Materials Science Division, Lawrence Berkeley National Laboratory. His research interest includes the synthesis of organic–inorganic hybrid nanomaterials, fundamental understanding of their structure–property relationships, as well as applications in high performance opto-electronic devices. He is a recipient of Office of Naval Research Young Investigator Award, Highly Cited Researcher in Cross-Fields, MIT Technology Review Innovators Under 35-China Award, and Materials Research Society Graduate Student Award.

Fig. 1 (a) Schematic representation of the 2D halide perovskites from different cuts of the 3D halide perovskite structure. L is a large organic cation, A is a regular cation such as Cs⁺ or methyl ammonium (MA⁺), B is a divalent metal cation, such as Pb²⁺ or Sn²⁺, and X is a halide. Reproduced from ref. 2 with permission from the Royal Society of Chemistry. (b) The possible energy level alignments for the alternating organic–inorganic 2D halide perovskites containing conjugated organic cations are shown, with arrows and dashed lines indicating the overall bandgap.

inorganic slabs usually serve as the potential wells while the organic layers function as the potential barriers. The well layers and width of the barrier can be easily adjusted by changing the number of perovskite sheets and the length of the organic cations. These important modifications are implemented by simply changing the composition or stoichiometry of the inorganic and organic salts precursors in the solution used to prepare hybrid crystals or thin films.

There have been a large number of reports regarding 2D perovskites that incorporate insulating aliphatic ammonium cations. For aliphatic, or even single-ring aromatic cation-based perovskites, the conduction band of the inorganic layers is substantially below that of the organic layers, and the valence band of the inorganic layers is similarly above that of the organic layers. Therefore, the inorganic sheets act as quantum wells for both electrons and holes. The organic cations form large energy barriers that hinder efficient charge transport; they solely play a structure-directing role in determining the properties of the perovskite. Conversely, semiconducting organic cations can play a more functional role in tuning the overall optical and electronic properties of perovskites. In principle, other types of band alignments can be achieved if semiconducting organic building blocks can be introduced into the hybrid crystal lattice (Fig. 1b). If conjugated organic cations with smaller energy gaps between the highest occupied molecular orbital (HOMO) and the lowest unoccupied molecular orbital (LUMO) are integrated with metal halide inorganic sheets having a larger bandgap, the barrier and well layers can be reversed (*i.e.*, type I in Fig. 1b). Alternatively,

the bandgaps for the organic and inorganic layers can be offset, leading to a type II heterostructure in which the wells for the holes and electrons are in different layers. Achieving such diverse structures and band alignments could potentially lead to a variety of high-performance optoelectronic devices with improved charge transport properties and stability. Furthermore, the incorporation of bulky and rigid conjugated ligands may further improve the stability of the perovskite materials, making them appealing for practical applications.

The general synthesis and application of 2D perovskites, particularly the RP phase 2D perovskites with aliphatic ligands, have been reviewed heavily by a number of groups, and therefore, they will not be covered in this work.[1,2,7–11] In this article, we focus on the recent progress on the synthesis, characterization, and device applications of novel 2D halide perovskites incorporating semiconducting conjugated organic ligands. In addition, we provide a short perspective on promising future directions of this type of organic–inorganic hybrid semiconductor materials. We believe that merging the organic electronics field with the halide perovskite electronics field will provide us unprecedented opportunities for the future of materials research.

2. Molecular design of conjugated ligands

Initially, most layered organic–inorganic halide perovskites contained simple aliphatic or single ring aromatic cations.[11]

3402 | *Mater. Chem. Front.*, 2020, **4**, 3400–3418

This journal is © The Royal Society of Chemistry and the Chinese Chemical Society 2020

A layered halide perovskite containing a phenyl-ethylammonium (PEA) cation was first synthesized in the 1990s and then become widely used in solar cells and LEDs.[12] However, further functionalization, using more complex conjugated structures, was found to be difficult. In principle, conjugated organic molecules can be incorporated into perovskites if two major criteria are fulfilled. First, an appropriate tethering terminal cation that can ionically bond to the inorganic sheet must be present. It is usually a protonated primary amine (e.g., ethylammonium). Second, π-conjugated backbones with small cross-sectional areas are needed in order to fit into the perovskite lattice appropriately.[11] Following these design principles, most conjugated organic ligands from the pool shown in Fig. 2 can be classified into three subgroups based on their structures: (1) phenyl ring-containing ligands (compounds 1 to 12),[13–22] (2) thiophene ring-containing ligands (compounds 13 to 20),[23–26] and (3) conjugated polymer-based ligands (compounds 21 to 24).[27–31]

2.1 Phenyl rings containing ligands

After investigations of halide perovskites based on PEA ligands, researchers introduced fused benzene rings into 2D hybrid perovskites. In 1998, a naphthalene-chromophore was incorporated into lead bromide-based perovskites, and it exhibited enhanced-phosphorescence that was caused by the energy migration from the exciton state of the inorganic layer to the excited triplet state of the naphthalene-chromophore.[13] A similar example was reported using pyrene as a light-emitting chromophore in Pb-based perovskites. By changing the halide from chloride to bromide, and to eventually iodide, it was observed

that the phosphorescence intensity increased significantly.[14] This was attributed to the external heavy-atom effect. Also, mixed halide perovskites were discussed and the excitonic band of the inorganic layer was shifted continuously by changing the ratio of chloride and bromide in layered perovskite ($C_{16}H_9$–CH_2–NH_3)$_2$PbCl$_n$Br$_{4-n}$. More recent work used organic ligands as the luminophore in order to target light-emitting devices. 2,3-Naphthalimide-ethylammonium molecules (NAAB) were doped into PEA-containing 2D lead-bromide perovskites and successfully increased the luminance of the 2D perovskites.[18] Another candidate for phenyl ring-based ligands, 4-biphenyl-methylamine (BPMA) was also incorporated into lead-bromide 2D perovskites.[17] By introducing the BPMA ligand, triplet excitons were extracted from the inorganic layer to generate room-temperature phosphorescence. This work suggests the organic ligands are indeed playing an important role in determining the optical properties of the hybrid material.

When designing organic ligands for 2D perovskites, one key parameter is the linker length between the aromatic moieties and terminal ammonium group. The spacing between those two molecular constituents has a significant impact on the optoelectronic properties of the hybrid perovskite materials. For example, a recent study on a naphthalene-containing lead bromide perovskite showed that the inter-layer spacing increases when the length of alkyl linking group increases.[13] At the same time, the relative intensity of the exciton emission also increased when the alkyl chain length of the naphthalene-linked ammonium molecules was increased. Different alkyl chain lengths were also incorporated into
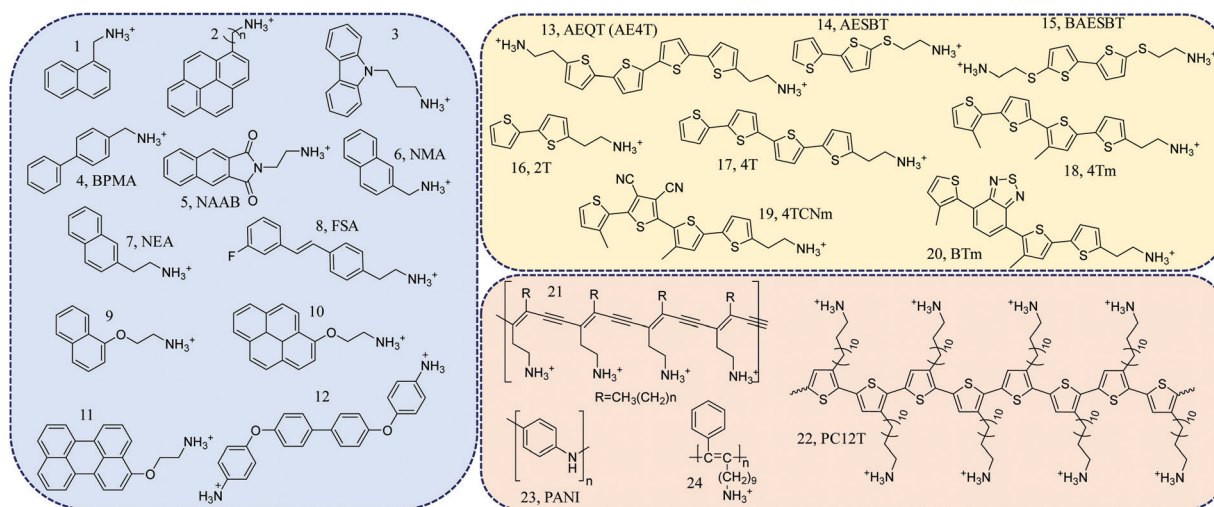
Fig. 2 Representative conjugated organic ligands for 2D halide perovskites: 1, naphthylmethyl ammonium;[13] 2, 1-pyrenylmethyl-ammonium (n = 1) and 1-pyrenylbutyl-ammonium (n = 4);[14,15] 3, carbazole-linked ammonium;[16] 4, 4-biphenylmethylammonium (BPMA);[17] 5, 2,3-naphthalimide-ethylammonium molecule, (NAAB);[18] 6, 1-(2-naphthyl)methanammonium (NMA);[19] 7, 2-(2-naphthyl)ethanammonium (NEA);[19] 8, 2-(4-(3-fluoro)-stilbenyl)ethanammonium (FSA);[20] 9, naphthalene-O-methylammonium;[21] 10, pyrene-O-ethylammonium;[21] 11, perylene-O-ethylammonium;[21] 12, 4,4′-(1,1′-biphenyl-4,4′-diyldioxy)dianiline;[22] 13, 5,5′′′-bis(aminoethyl)-2,2′:5′,2′′:5′′,2′′′-quaterthiophene (AEQT);[23] 14, 5-ammoniummethylsulfanyl-2,2′-bithiophene (AESBT);[24] 15, 5,5′-bis(2-phthalimidoethylsulfanyl)-2,2′-biothiophene (BAESBT);[24] 16, 2-([2,2′-bithiophen]-5-yl)ethylammonium (2T);[25] 17, 2-([2,2′:5′,2′′:5′′,2′′′-quaterthiophen]-5-yl)ethylammonium (4T);[25] 18, 2-(3′′′,4′-dimethyl-[2,2′:5′,2′′:5′′,2′′′-quaterthiophen]-5-yl)ethylammonium (4Tm);[25,26] 19, 2-(3′′,4′′-dicyano-3′′′,4′-dimethyl-[2,2′:5′,2′′:5′′,2′′′-quaterthiophen]-5-yl)ethylammonium (4TCNm);[25] 20, 2-(4′-methyl-5′-(7-(3-methylthiophen-2-yl)benzo[c][1,2,5]thiadiazol-4-yl)-[2,2′-bithiophen]-5-yl)ethylammonium (BTm);[25] 21, poly(deca-3,5-diyn-1-ammonium(DDA));[27,28] 22, poly(3-aminododecylthiophene) (PC12T);[29] 23, polyaniline (PANI);[30] 24, poly(11-phenyl-10-undecyn-1-ammonium).[31]
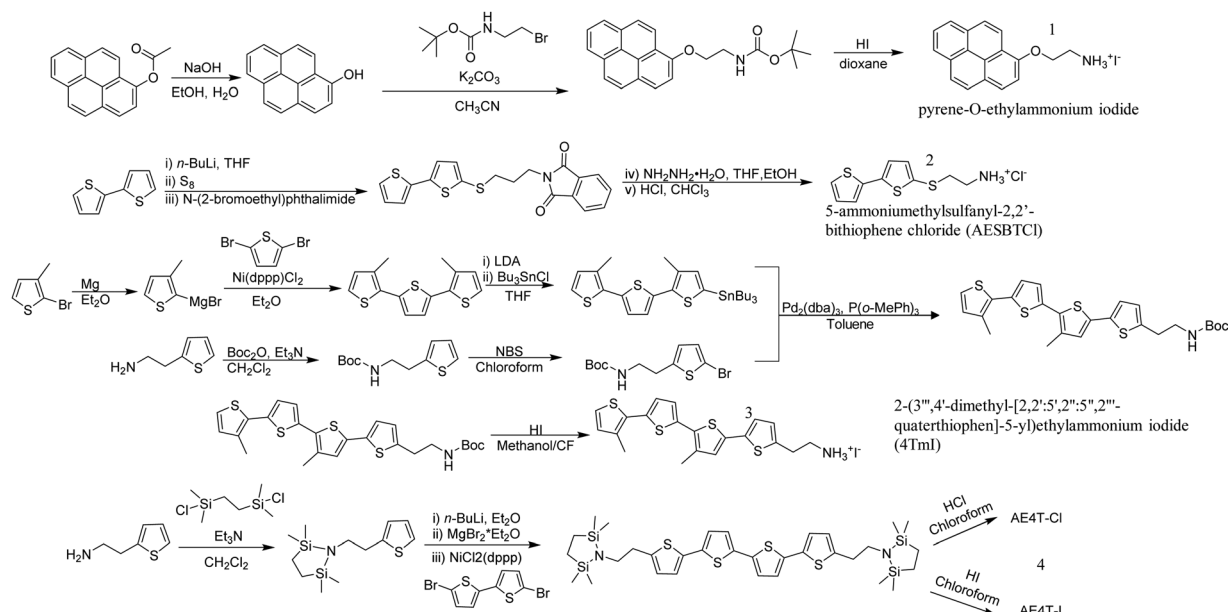
Fig. 3 Representative synthetic pathways for conjugated organic ligands: **1**, pyrene-*O*-ethylammonium iodide;[21] **2**, 5-ammoniumethylsulfanyl-2,2′-bithiophene chloride (AESBTCl);[24] **3**, 2-(3‴,4′-dimethyl-[2,2′:5′,2″:5″,2‴-quaterthiophen]-5-yl)ethylammonium iodide (4TmI);[25,26] **4**, AE4T based salts.[32]

carbazole-liked ammonium bromides.[16] The ligands with methylene chains of three-, four-, or five-carbon linkers were inserted into lead-bromide perovskites to fabricate thin films. The perovskite films with three and four carbon linkers showed broad, low intensity, and blue-shifted exciton absorption peaks, indicating that the perovskite structures were disturbed. In contrast, the thin film with a five-carbon linker had sharp and intense exciton absorption, suggesting a better-defined perovskite structure was formed. Mitzi *et al.* reported similar observations on naphthalene-containing ligands 1-(2-naphthyl)methanammonium (NMA) and 2-(2-naphthyl)ethanmmonium (NEA) ligands in 2D Pb-based perovskites.[19] They successfully grew perovskite single crystals with those ligands. The ligand penetration depth – defined as the distance between the nitrogen atoms of the organic cation and the plane of the axial halogen atoms of the perovskite sheet – was investigated. It shows that with longer alkyl chain length, the ammonium terminal group penetrated deeper into the inorganic framework, caused larger Pb–halide–Pb angles and eventually altered the band structure. Additionally, hydrogen bonding strength is also correlated to the penetration depth of the ammonium terminal group in this perovskite system. When the penetration is around 0.4 Å, strong hydrogen bonding interactions occurred. These studies clearly indicate that a proper linker length is essential for the synthesis of high quality 2D hybrid perovskite materials.

Most of the previously-mentioned organic ligands are commercially available, but the limited number of choices hindered the design of functional organic ligands and the control of the alkyl linker group lengths. Stupp *et al.* designed a novel synthetic pathway with 1-napthol, hydroxyl-pyrene and hydroxyl-perylene on one side and brominated alkyl linkers with different lengths on the other side to cross couple a series of aromatic-*O*-linker-NH₃I ligands (Fig. 3).[21] This strategy provided an efficient way of introducing π-conjugated moieties into 2D perovskites. It is worth noting that the oxygen in the ether linkage in those organic ligands can form intramolecular hydrogen bonds with ammonium cation, influencing the extension of the alkyl linker and eventually the optical bandgap.

2.2 Thiophene rings containing ligands

Thiophene-containing organic molecules have played an important role in organic semiconductors because of their versatility, tunability, and availability. The sulfur-containing thiophene ring offers active reaction sites for making large conjugated molecules with facile chemistry. In addition, oligothiophene and polythiophene are excellent hole-conducting materials that have been widely used in organic electronics. However, only a sparse number of conjugated thiophene-based organic ligands have been incorporated into 2D halide perovskites. Notably, Mitzi *et al.* incorporated oligothiophene with two alkylammonium tethering groups into Pb-based 2D perovskites and obtained corresponding single crystals.[23] The molecular design of this conjugated thiophene ligand followed the two major criteria mentioned above. That is, (1) two relatively short ethylammonium tethering groups were utilized at the two ends of the molecule to help stabilize the perovskite framework, and (2) the linear quaterthiophene unit is narrow enough to fit into the perovskite lattice. One more consideration of using the quaterthiophene backbone is that the peak optical absorption is close to lead-iodide layered perovskites exciton peaks (at around 510 nm). Therefore, electronic transitions between the organic and inorganic layers in this hybrid perovskite system are likely to occur. Following on this work, Mercier *et al.* studied the effect of mono- *versus* diammonium bithiophene organic ligands in Pb-based 2D perovskites.[24]

A Kumada coupling reaction was applied to synthesize mono- and diammonium bithiophene cations (Fig. 3). When two ligands were incorporated into Pb-based perovskites, only the diammonium cation formed the RP-phase perovskite. For the monoammonium cation, a zig-zag inorganic framework was surrounded with organic ligands in a head-to-tail arrangement. This is different relative to the diammonium cation, which forms hydrogen bonds on both sides of the ligand to help stabilize the perovskite sheet. Because the monoammonium cation forms hydrogen bonds in a weaker manner and because of the π–π interactions between ligands in solution before crystallizations, the formation of the RP-phase 2D perovskites are hindered.

To address the difficulty of synthesizing RP-phase 2D perovskites, our group designed and synthesized a series of thiophene-containing conjugated organic ligands and single crystalline organic–inorganic Pb-based 2D halide perovskites were obtained.[25] Asymmetric monoammonium cations were implemented instead of diammonium cations to help control surface chemistry. The monoammonium cations also inhibit out-of-plane and promote in-plane crystal growth. Additionally, bulky and hydrophobic monoammonium cations sandwiched the inorganic framework to provide protection for the inorganic layer and improved the stability of the 2D perovskite towards moisture. Those ligands, starting from 2-([2,2′-bithiophen]-5-yl)ethylammonium (2T) ligand containing two thiophene rings to 2-([2,2′:5′,2″:5″,2‴-quaterthiophen]-5-yl)ethylammonium (4T) ligand consisting of four thiophene rings, were all synthesized using palladium catalyzed Stille coupling reactions. During the preparation of the 2D halide perovskite, strong π–π interactions between ligands and poor solubility were observed for the 4T ligand. To overcome ligand self-aggregation and self-crystallization, two methyl groups were introduced on the backbone to make a new 2-(3‴,4′-dimethyl-[2,2′:5′,2″:5″,2‴-quaterthiophen]-5-yl)ethylammonium (4Tm) ligand (Fig. 3). The strong packing between ligands was suppressed to form bulk crystals of 4Tm-containing Pb-based 2D halide perovskite. Under this molecular design paradigm, a small band-gap chromophore unit, 2,1,3-benzothiadiazole, was inserted to make the BTm ligand and two strong electron-withdrawing cyano groups were introduced to make the 4TCNm ligand. Like the 4T ligand, the bulk crystal of the 4TCNm ligand, Pb-based perovskite was not obtained due to the steric hindrance of two cyano groups as well as self-aggregation.

The hydrophobic nature of organic molecules makes them good candidates as encapsulation layers to protect the perovskite framework. Tin(II)-based perovskites suffer from stability issues because Sn^{2+} can be easily oxidized to Sn^{4+} in ambient conditions. As such, several large and bulky organic ligands have been introduced to serve as protecting layers. In addition to Loh's work that used a stilbene derivative as the organic ligand to improve the stability of tin(II)-based 2D perovskites,[20] the 4Tm ligand also was incorporated to synthesis tin(II)-based perovskite bulk crystals and the perovskite structure can be well maintained for more than a month in ambient conditions.[26] Bulky monoammonium cations, like (2-(4-(3-fluoro)stilbenyl)ethanammonium) (FSA) and 4Tm,

uniformly covered the Sn-based inorganic sheet to prevent moisture and oxygen penetration and provided enhanced ambient stability compared with Sn-based perovskites with simple butyl-ammonium or PEA ligands.

2.3 Conjugated polymer-based ligands

Among semiconducting materials, conjugated polymers play an important role because of their structural diversity and tunable bandgaps. Proper bandgap alignment of conjugated polymers with inorganic parts in hybrid perovskites can bring interesting charge and/or energy transfer interactions.[1] The incorporation of polymeric species in 2D halide perovskites can also have positive effects on the stability and mechanical properties of the materials. In 2001, polydiacetylene was first introduced into 2D halide perovskites and a hybrid exciton feature was observed from the hybrid perovskite thin films.[27] Later work from Solis-Ibarra et al. formed the same system using a simple thermal treatment, and it is possible to dope the formed polydiacetylenes inside the perovskites with oxygen or iodine, which results in a drastic improvement of light absorption and conductivity.[28] Polymers with conjugated aromatic rings as backbones were introduced into 2D halide perovskites, including amphiphilic poly(thiophene)s,[29] polyaniline,[30] and phenyl-substituted polyacetylene.[31] Tang et al. synthesized a disubstituted polyacetylene with a hidden amino functionality and then hydrolyzed and quaternized this group to make an ammonium salt. After mixing with lead bromide, they fabricated a thin film that emitted a blue light with high quantum yield. This strategy opened the potential of combining semiconducting polymers and perovskites to make functional light-emitting devices.

Although several attempts have been made to design and synthesize semiconducting polymer-containing 2D perovskites, it is still a large challenge to synthesize this type of perovskite with confirmed single crystal structures. Most of the reported studies are based on perovskite thin films with moderate crystallinity. From a synthetic point of view, it is hard to introduce tethering groups on polymer backbones because the length of tethering groups is crucial to perovskite formations. Furthermore, in situ polymerization processes often require special conditions like UV irradiation, active center initiations or high temperature with high pressure. During polymerization, active species (e.g., radicals, ions, and water) can be generated, which possibly destroys the ionic perovskite structures. Therefore, a clear opportunity for future research is to undertake next-generation strategies, as they are required for further advancing this particular approach.

3. Optical and electronic properties

3.1 Bandgap and band alignment tunability

The bandgap of 2D perovskites can be tuned through halide substitution as it is done in 3D hybrid perovskites. Replacing iodine with bromine or chlorine will result in an increase in the bandgap, and mixed halide alloys can be employed to further tailor the optical and electronic properties.[33] The properties of

This journal is © The Royal Society of Chemistry and the Chinese Chemical Society 2020

Mater. Chem. Front., 2020, 4, 3400–3418 | 3405

2D perovskites can be further tuned through metal substitutions. Compared to their Pb-based counterparts, Sn-based 2D perovskites typically have smaller optical gaps, and hence, PL emissions usually occur at wavelengths longer than 600 nm. Interestingly, the presence of F atoms in the FSA ligand breaks the trend and blue shift the PL emission for $n = 1$ homologue.[20]

The role that the organic cations play in dictating octahedral distortion, and thus, the optical properties of layered perovskites has been previously corelated to the position of the positively charged ammonium cation with respect to the negatively charged inorganic lattice. A reduction of the metal–halide–metal bond angle from the ideal value of $180°$ alters the band structure, and this will increase the bandgap. A recent study found that, for 2D lead halide perovskites containing aromatic cations, the length of the alkyl tether connecting the ammonium cation to the aromatic moiety has a much larger effect on the bandgap than the number of aromatic rings on the cation.[19] Compared to the ethyl tether, the methyl tether results in more strain and a smaller Pb–X–Pb (X = Cl, Br, I) bond angle. Likewise, specifically-designed conjugated organic cations could modify the structure of the inorganic framework and tune the optical and electronic characteristics as well. For example, a series of $n = 1$ layered halide perovskites were reported with the form (aromatic-O-linker-NH$_3$)$_2$PbI$_4$ where the conjugated moiety is naphthalene,

pyrene, or perylene, the O represents an oxygen atom, and the linker is an ethyl, propyl, or butyl carbon chain. Optical absorption spectroscopy was used to determine the energy of the S$_1$ exciton peak (E_{S_1}) in thin film samples of each layered perovskite. It was observed that the E_{S_1} values increase linearly with decreasing average cationic nitrogen to peripheral-iodide distance (d_{N-I}), as shown in Fig. 4.[21] As the d_{N-I} decreases, the electrostatic interaction between the cationic nitrogen and negatively charged inorganic lattice increases, resulting in a more severe octahedral distortion and a higher E_{S_1}. The structural features of the organic cation must dictate d_{N-I} and thus influence the resulting electrostatic interaction. Evidenced in their crystal structures, the intramolecular hydrogen bonding increases d_{N-I}, and reduces the optical bandgap. Additionally, these materials exhibit enhanced out-of-plane conductivity, owing to the better energy level matching between the inorganic and organic layers. These results demonstrate that the structure of the organic cation influence the electronic properties of the resultant perovskites and suggests that the properties can be tuned by changing the d_{N-I} through steric control and intramolecular interactions.

Apart from the above structural role, another important feature of semiconducting conjugated organic cations is their tunable bandgap and energy levels, which are comparable to
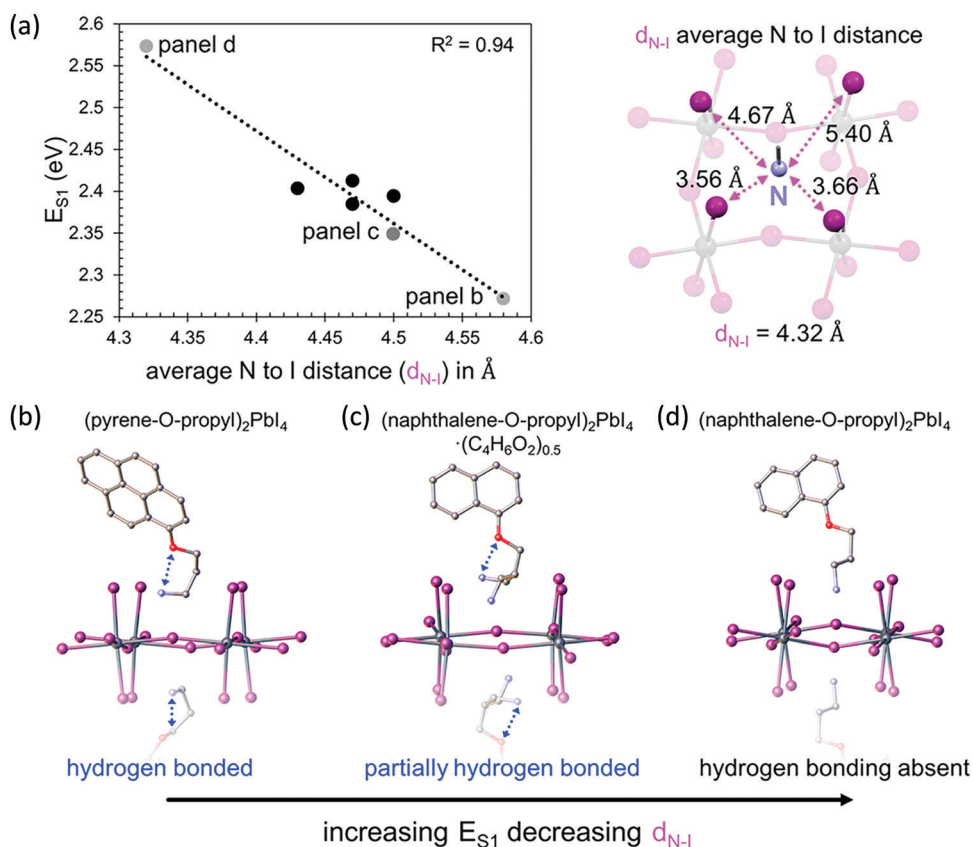
Fig. 4 (a) Energy of the S$_1$ exciton *versus* average distance between the nitrogen cation and the peripheral iodides of the inorganic layers (d_{N-I}) (left); (naphthalene-O-propyl-NH$_3$)$_2$PbI$_4$ structure showing with dashed lines the four different N–I distances used to calculate d_{N-I} (right). Crystal structures showing intramolecular hydrogen bonding (if present) for (b) (pyrene-O-propyl-NH$_3$)$_2$PbI$_4$, (c) (naphthalene-O-propyl-NH$_3$)$_2$PbI$_4$·(C$_4$H$_6$O$_2$)$_{0.5}$, and (d) (naphthalene-O-propyl-NH$_3$)$_2$PbI$_4$. Reproduced with permission from ref. 21. Copyright 2018, American Chemical Society.

3406 | *Mater. Chem. Front.*, 2020, **4**, 3400–3418

This journal is © The Royal Society of Chemistry and the Chinese Chemical Society 2020

inorganic perovskite sheets. For band structure calculations of 2D halide perovskites semiconductors based on π-conjugated oligothiophene cations (AEnT^{2+}, where n signifies the number of thiophene rings in the chain), Blum *et al.* employed large-scale hybrid density functional theory with spin–orbit coupling.[34] They predicted quantitatively how varying the organic and inorganic component allows for control over the nature, energy, and localization of carrier states in a quantum-well-like fashion. Their first-principles predictions show that the interface between the organic and inorganic parts within a single hybrid can be modulated systematically, enabling the selection between different type I and type II energy level alignments (Fig. 5). Theoretical studies on the electronic properties of (AE4T)BX$_4$ (B = Pb, Sn; X = Cl, Br, I) have also been conducted recently. The location of frontier orbitals varies according to the different halides and metal cations with bandgaps varying from 2.06 eV to 2.68 eV (Fig. 5d).[35] Such tunability of electronic properties, especially the energy level alignments of the organic and inorganic components, opens the possibility of controlling the charge separation or recombination processes at the organic–inorganic interface. All these computational results are consistent with the experimental results using AE2T and AE4T (AEQT) ligands.[23,32] In their optical absorption spectra, the exciton features from the metal halide sheets along with characteristic absorption from the chromophores can both be identified.

Recently, we experimentally realized the tunability between the different type I and type II energy level alignments mentioned above in 2D lead halide perovskites by designing a series of conjugated organic cations.[25] Their band alignments were clarified and qualitatively depicted by using ultraviolet photo-electron spectroscopy (UPS) and cyclic voltammetry (CV). Fig. 6 shows optical and PL images of the corresponding self-assembled nanocrystals. The PL result of (2T)$_2$PbI$_4$ is consistent with a type I heterojunction and energy transfers efficiently to the lowest energy emitter. We then introduced a small bandgap chromophore, 2-(4′-methyl-5′-(7-(3-methylthiophen-2-yl)benzo[c]-[1,2,5]thiadiazol-4-yl)-[2,2′-bithiophen]-5-yl)ethylammonium (BTm).

The new 2D perovskite (BTm)$_2$PbI$_4$ exhibits a reversed type I heterojunction. Its PL signal originates from the organic BTm layers. For (4Tm)$_2$PbI$_4$ and (4TCNm)$_2$PbI$_4$, where 4TCNm is 2-(3″,4″-dicyano-3′′′,4′-dimethyl-[2,2′:5′,2″:5″,2′′′-quaterthiophen]-5-yl)ethylammonium, the HOMO–LUMO and inorganic bands are staggered to form type II heterojunctions, the introduction of two strong electron withdrawing cyano groups also enabled the inversion of the energy level offset between organic and inorganic layers. Subsequently, emissions from both the inorganic layer and the organic layers are 99.9% quenched, suggesting efficient charge separation at the interface. The charge transfer time, around 10 ps, and long-lived charge-separated state over the nanosecond time scale in these systems were further demonstrated using time-resolved photoluminescence and transient reflection spectroscopy.[36] From these computational and experimental results, one could expect energy/charge transfer between organic and inorganic components in 2D halide perovskites by bandgap engineering of conjugated compounds, and this can bring interesting electronic structures and properties.

3.2 Room temperature phosphorescence

Incorporation of semiconducting conjugated organic cations will lead to an additional subtlety because of the participation of the triplet states in organic layers, enabling another unique behavior in these 2D hybrid quantum well systems. For example, band alignment may favor exciton transfer through inorganic bands to organic triplet states and result in phosphorescence. Generally, the transition from the singlet S$_0$ state to triplet T$_1$ state in conjugated organic cations is spin-forbidden, and there is no resonance coupling between the organic layers and inorganic layers in 2D halide perovskites. In 2008, Era *et al.* verified that the triplet–triplet Dexter-type energy transfer (DET) from Wannier excitons in inorganic lead bromide perovskite layers to the triplet state of the naphthalene molecules is effective and, due to quite fast relaxation in the fluorophore vibronic band, the back transfer from the organic layers does not occur.[37] DET is a process in which the donor and acceptor
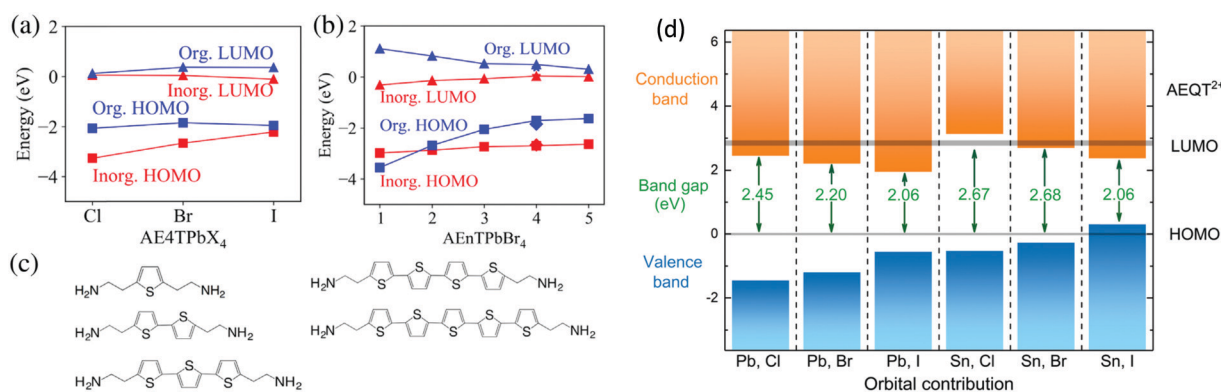
Fig. 5 (a) Frontier energy levels of the organic and inorganic components at the Γ point among the series of AE4TPbX$_4$ (X = Cl, Br, I). (b) Frontier energy levels at the Γ point among the series of AEnTPbBr$_4$ (n = 1–5). (c) Oligothiophene-based organic molecules considered in the all-anti configuration for varying the number n. (d) Orbital contribution near the band edge of (AEQT)BX$_4$ (B = Pb, Sn; X = Cl, Br, I) series, where the HOMO of AEQT^{2+} is set to 0 eV. The LUMO and HOMO is represented by grey shadow, of which thickness indicate the energy range of the orbitals. Figures reproduced with permission from: (a–c), ref. 34. Copyright 2018, American Physical Society; (d) ref. 35. Royal Society of Chemistry.
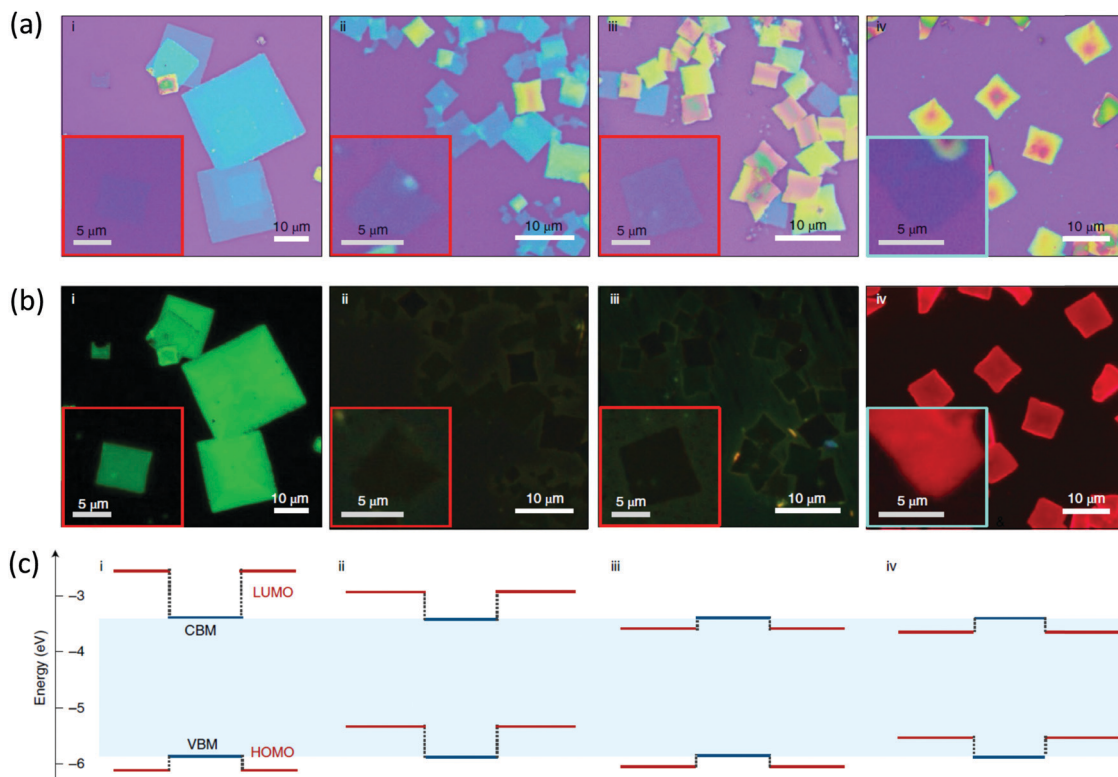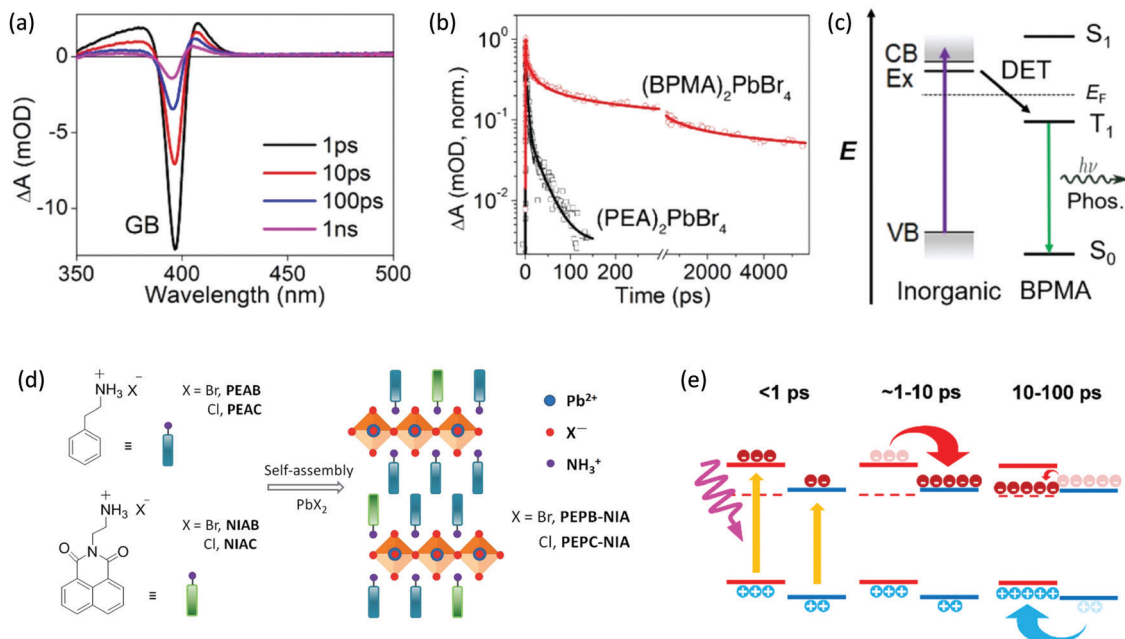
Fig. 6 Optical properties of the hybrid halide perovskites quantum wells. (a) Optical microscopy images of the assembled 2D crystals grown on SiO_2/Si substrates: $(2T)_2PbI_4$ (i), $(4Tm)_2PbI_4$ (ii), $(4TCNm)_2PbI_4$ (iii) and $(BTm)_2PbI_4$ (iv). The insets are images for monolayer-thick single-quantum-well structures. (b) The corresponding PL images of the assembled 2D crystals under ultraviolet excitation. (c) The corresponding energy level alignments (relative energy levels) of organic (dark red lines) and inorganic (dark blue lines) layers within the hybrid 2D perovskites. Reproduced from ref. 25 with permission from the Springer Nature.

exchange their electrons bilaterally. Unlike Förster resonant energy transfer (FRET), the DET mechanism does not involve a direct transition from the ground state to the excited state in the acceptor, allowing the triplet transfer with the electron exchange process. The transfer rate constant of DET exponentially decays as the distance between these two parts increases. Hence, intimate contact between the organic cations and inorganic layers is also required to allow efficient direct electron exchange *via* the Dexter mechanism. Phosphorescence was also observed in several other examples, including naphthalene and pyrene derivatives, within lead halide frameworks.[13,14,38] Recently, 2D halide perovskite based on a 4-biphenylmethylamine (BPMA) cation with low-lying triplet energy levels has successfully extracted triplet excitons from the inorganic component, thereby generating room temperature phosphorescence.[17] As shown in Fig. 7a–c, time-resolved spectroscopy confirms DET from excitons in the inorganic layers to the molecular triplet states. Efficient phosphorescence at room temperature was achieved with a long lifetime of several milliseconds. In this way, a wide range of emission colors can be achieved by facile molecular design of organic cations.

Room temperature phosphorescence also can occur by doping an organic fluorophore into the organic cations of 2D halide perovskites (Fig. 7d). Yellow phosphorescence of 1,8-naphthalimide (NI) is obtained in thin films and powders

in air with this doping protocol.[39] The triplet excitons of NI are mainly derived from Wannier excitons of inorganic perovskites through energy transfer for films, and from singlet excitons of NI through intersystem crossing for powders. The quantum yield, lifetime, and exact emission wavelength of the phosphorescence can be tuned by changing the halide and fluorophore in the perovskites, as well as their solid morphology.

Phosphorescence does not only happen in type I heterojunction of halide perovskites. In the type II heterojunction case, besides the quenched photoluminescence, for appropriately selected organic/inorganic components, it is possible to subsequently reform excitons in the organic triplet states. Although the singlet–triplet transition is forbidden in the neat conjugated organic compounds, it can be enabled in the hybrid material if the carriers cascade through certain inorganic states. Recently, this process has been found in the $(AEQT)PbI_4$ system as shown in Fig. 7e.[32] Because triplet states in oligothiophenes generally do not lead to efficient phosphorescence, PL measurements are inferior to transient absorption spectroscopy for tracking excitations in oligothiophene-based perovskites or other hybrid materials with weak triplet emission. In this sense, the resulting hybrid 2D halide perovskite structures may transcend the traditional inorganic quantum well model and involve synergistic organic–inorganic interactions.

3408 | *Mater. Chem. Front.*, 2020, **4**, 3400–3418

This journal is © The Royal Society of Chemistry and the Chinese Chemical Society 2020

Fig. 7 (a) TA spectra of the $(BPMA)_2PbBr_4$ thin film with 330 nm pump, photon fluence of 73 μJ cm^{-2}. (b) Decay of the GB peak for $(BPMA)_2PbBr_4$ and $(PEA)_2PbBr_4$, note the break on X-axis separating the time scale into hundreds of ps and ns. (c) Schematic illustration of the DET process between the inorganic layer and BPMA cation in $(BPMA)_2PbBr_4$, which results in phosphorescence. (d) Synthesis and structural illustration of the doped perovskites. (e) schematic of carrier transfer in $AE4TPbI_4$, wherein organic and inorganic parts are indicated in red and blue lines, the triplet state of AE4T is represented by the dashed red line. Figures reproduced with permission from: (a, b and c), ref. 17. Copyright 2019, American Chemical Society; (d) ref. 39. Royal Society of Chemistry; (e) ref. 32. Royal Society of Chemistry.

3.3 Other promising functionalities

The broad range of available conjugated organic cations for 2D halide perovskites provides a convenient way to alter and tune the optoelectronic properties of the hybrid materials. There are now numerous examples wherein the organic cation is more functional, therefore enabling a more diversified role in the optoelectronic properties of the hybrids.

The molecular packing and conformation in the hybrid crystal lattice have not been well understood. For example, a herringbone arrangement of the oligothiophene ligands was found in several materials [e.g., $(AEQT)PbI_4$ and $(4Tm)_2PbI_4$], which prevents direct π–π stacking between the molecules.[23,25] In the case of $(AEQT)PbI_4$, the quaterthiophenes adopt an unusual, nearly planar cis–trans–cis conformation between adjacent thiophene rings. This conformation is presumably favored by the hydrogen bonding and aromatic edge-to-face interactions holding the molecules in the framework.[23] However, the quaterthiophenes in $(4Tm)_2PbI_4$ adopt an all-trans configuration.[25] This is probably because the monoammonium ligands have more freedom to rotate to find the confirmation with lowest energy; but for the AEQT diammonium ligands, the two ends are all ionically bonded to the inorganic layers and molecules are forced into an energetically less favorable conformation. New molecular design principles need to be developed to better control the spatial arrangement of the molecules and their associated electronic properties.

These unique interactions of conjugated cations and their rigid, rod-like nature impart them another functionality (i.e., they can act as templates to stabilize unusual 2D halide perovskite phases that are often inaccessible using traditional spacer cations). In 2000, the unique templating influence of AE4T in stabilizing an unusual Bi-deficient 2D halide perovskite was demonstrated. This material features 2D layers of corner-sharing distorted BiI_6 octahedra with randomly distributed Bi-vacancies and represents the first member of a new family of metal-deficient 2D HOIPs.[40] The intermolecular aromatic interactions of AE4T are strong enough to compensate for an otherwise unfavorable formation enthalpy. In another work, Wudl et al. synthesized a quasi-perovskite crystal containing tetrathiafulvalene and observed charge transfer between the organic and inorganic moieties.[41] The first example of a lead-free 2D mixed-metal double perovskite, (i.e., $(AE2T)_2AgBiI_8$) is also realized using the same strategy.[42] The metal site mixing, combined with the templating influence associated with AE2T, helps to stabilize the unprecedented iodide-based 2D double perovskite structure showing a direct bandgap of 2 eV. These examples proved the value of employing specifically designed conjugated templating organic cations to obtain unusual 2D halide perovskite phases, thus enriching their optical and electronic properties.

Two hybrid Ruddlesden–Popper compounds with a 2-(4-biphenyl) ethylammonium (BPEA) cationic spacer were prepared and reported to have slightly enhanced transient photoconductance over counterparts with n-butylammonium spacer cations.[43] It is unclear whether this increase is solely due to the presence of the conjugated moieties in cations, but it appears that the use of a higher dielectric constant organic spacer can improve the

This journal is © The Royal Society of Chemistry and the Chinese Chemical Society 2020

Mater. Chem. Front., 2020, **4**, 3400–3418 | **3409**

transport properties of RP perovskite materials. Similarly, in emerging chiral 2D halide perovskites, although it may not be the direct reason, incorporation of conjugated organic cations did enable better circular dichroism tunability.[44] Beyond the individual conjugated organic components, the formed poly-diacetylenes inside 2D halide perovskite can be further doped, which leads to the formation of radicals and the drastic improvement in light absorption and conductivity.[28] Besides, it is possible to assemble organic charge-transfer complexes in the organic layer of 2D layered perovskites. Charge-transfer complexes are reported to be formed in the organic layer of 2D layered perovskites using a pyrene-butylammonium ($PyrC_4$) donor and tetracyanoquinodimethane (TCNQ) or tetracyano-benzene (TCNB) acceptors.[45] Upon incorporation of TCNQ molecules in a 1:1 ratio with $PyrC_4$, to form ($PyrC_4$:TCNQ 1:1)$_2$PbI$_4$, a novel 2D layered perovskite containing charge-transfer complexes was reported, and incorporation of charge-transfer complexes is found to has a significant influence on the absorption in the visible wavelength region and emission spectra as well. Different combinations of donor and acceptor molecules can be used to tune the optoelectronic properties of the perovskite.

4. Device applications

4.1 Photovoltaic devices

Stability has been one of the major concerns of halide perovskites photovoltaics (PVs); thus, applying the more-stable 2D

halide perovskites to PVs is of significant interest. The insulating nature of traditional cation spacers affect the charge transport perpendicular to the inorganic layers. This problem can be addressed either by creating vertically-grown films using hot-casting or fast post-annealing techniques,[46,47] or by using high n number quasi-2D perovskites. The vertically-grown PV showed a PCE of 12.52% while maintaining high performance after exposure to moisture and light.[46] Quasi-2D perovskites, on the other hand, showed even higher PCE values, reaching 15.3% by increasing the n number greater than 10 while maintaining stability.[48–51] Although the trend in PCEs with increasing n numbers make these devices controversial with respect to their definition as 2D halide perovskites, the idea of using bulky ligands as a passivation method is clearly established,[52] and π-conjugated bulky ligands are found to show better passivation capability comparing to the alkyl counterparts. For instance, by employing the conjugated ligand 3-phenyl-2-propen-1-amine (PPEA) as a capping layer of 3D MAPbI$_3$, defects can be healed by the resulting 2D–3D architecture. This approach leads to a solar cell with PCE of 20.53% and enhanced stability.[53,54] Furthermore, the complex π-conjugated ligands could act as active electronic components that provide better out-of-plane charge transport (Fig. 8a). Enhanced charge transport has been demonstrated by incorporating a series of complex aromatic ligands that resulted in enhanced out-of-plane conductivity.[21] Compared to common alkyl (BA)$_2$PbI$_4$, the (pyrene-O-propyl-NH$_3$)$_2$PbI$_4$ showed orders of magnitude higher out-of-plane conductivity, and the resulting PVs had an average PCE of 1.14%, which is the best for n = 1 2D Pb-based halide perovskites at the moment. The higher
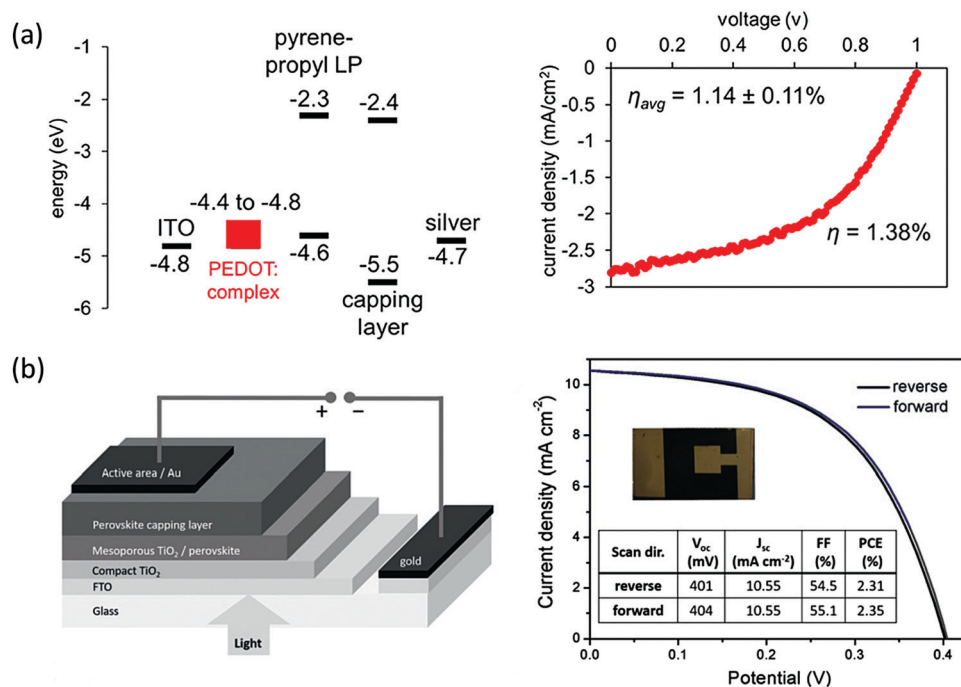
Fig. 8 (a) Energy levels of the layers in the (pyrene-O-propyl-NH$_3$)$_2$PbI$_4$ layered perovskite solar cell and I−V curve for the champion device with 1.38% efficiency. (b) Schematic representation of the device configuration and photovoltaic performance of the champion device using Bn$_2$SnI$_4$ pure 2D perovskite. Figures reproduced with permission from: (a) ref. 21. Copyright 2018, American Chemical Society; (b) ref. 55. Copyright 2019, Wiley-VCH.

3410 | *Mater. Chem. Front.*, 2020, **4**, 3400–3418

This journal is © The Royal Society of Chemistry and the Chinese Chemical Society 2020

conductivity is attributed to the better energy level alignment with perovskite conduction band and valence band. The use of symmetrical imidazolium-based cations such as benzimidazolium (Bn) and benzodiimidazolium (Bdi) allow for the formation of 2D halide perovskites with relatively narrow bandgaps compared to traditional $-NH_3^+$ amino groups, with optical bandgap values of 1.81 eV and 1.79 eV for Bn_2SnI_4 and $BdiSnI_4$ respectively.[55] Using Bn_2SnI_4, lead- and HTM-free stable 2D Sn-based halide perovskite solar cell was then demonstrated, and preliminary efforts in the devices show promising efficiencies of up to 2.3% (Fig. 8b). With this exciting progress, a way forward in 2D halide perovskites PVs is to combine the high ambient tolerant of π-conjugated bulky ligands with the vertical aligned 2D halide perovskites synthesis. To date, vertically-aligned 2D halide perovskites with conjugated ligands PVs have not been thoroughly studied and optimized. So far, vertically-aligned 2T based 2D halide perovskite PV with PCE ∼ 8% was fabricated only as a proof-of-concept device for the post annealing method.[47] With more studies in new conjugated ligands design and optimization, we expect to see 2D halide perovskites PVs with excellent performance and stability.

4.2 Field-effect transistors

Despite the rapid development of halide perovskites PVs, the progress in field-effect transistors (FETs) has been much slower. Bulk and interfacial defects, inefficient carrier injection, ion migration, and material degradation have hampered the fabrication of high-performance halide perovskites FETs, and as a result, only a scattered amount of reports exist.[56–59] Ion migration is especially an issue with halide perovskites FETs because it leads to misinterpretation of mobility and large

hysteresis caused by electric field screening.[57] 2D halide perovskites have shown potential in resolving these issues due to the superior stability and the suppressed ion migration. In fact, the first halide perovskites FET was based on a $n = 1$ 2D halide perovskite (i.e., $(PEA)_2SnI_4$) reported by Mitzi back in 1999, in which the device showed a hole mobility of 0.6 cm^2 V^{-1} s^{-1}.[60] Base on their results, the performance of $(PEA)_2SnI_4$ FET has improved recently, showing a hole mobility >10 cm^2 V^{-1} s^{-1}. This was achieved by application of a self-assembled monolayer (SAM) that enhance the carrier injection and the grain morphology (Fig. 9a).[61] However, $(PEA)_2SnI_4$ is still prone to degradation and requires additional encapsulation.[62] An alternative and more reliable solution is the introduction of novel conjugated organic cations. Recently, our group reported the quaterthiophene-based ligand (4Tm) that could tremendously strengthen the Sn-based 2D halide perovskites ambient and thermal stability.[26] Compared with the $(PEA)_2SnI_4$ device, which shows no performance after 1 day of storage in a glovebox, $(4Tm)_2SnI_4$ demonstrated high retention in FET performance after 30 days. This stability essentially results from the higher hydrophobicity of the 4Tm ligand and the increased formation energy of $(4Tm)_2SnI_4$. Furthermore, $(4Tm)_2SnI_4$ exhibited ten-fold improvement in hole mobility (2.32 cm^2 V^{-1} s^{-1}) comparing to $(PEA)_2SnI_4$ without a SAM and a suppressed hysteresis (Fig. 9b). The improved mobility is attributed to the active role of 4Tm ligand in hole injection from the contacts to the inorganic layers and the large grain size. It was also proposed that 4Tm ligand could suppress the ion migration better than PEA. These promising results indicate an exciting approach of high-performance halide
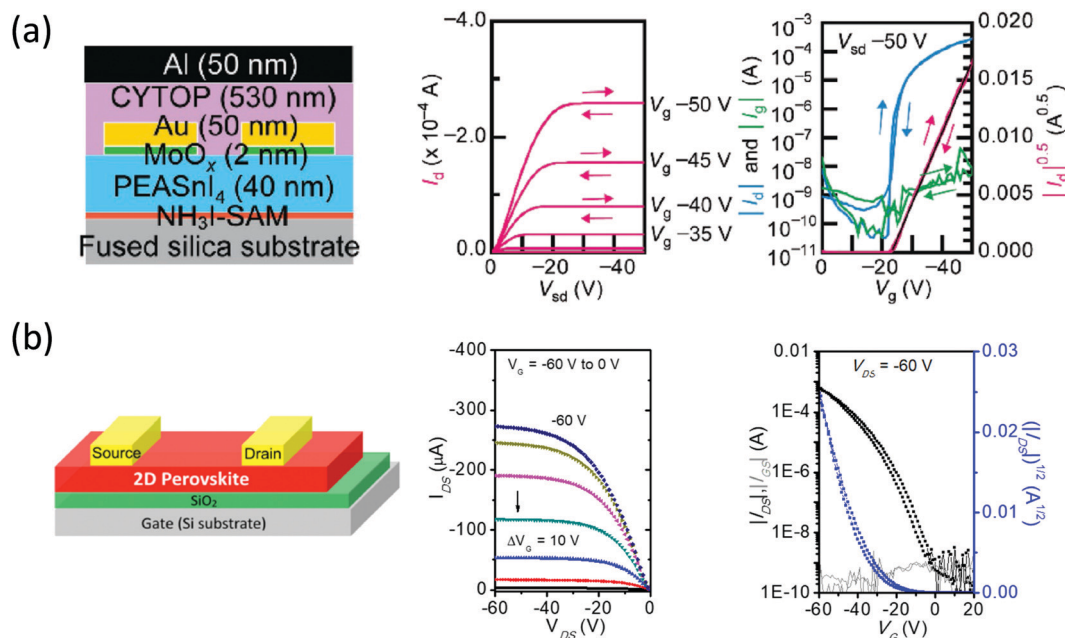
Fig. 9 (a) Schematic representation of the device configuration of $(PEA)_2SnI_4$ based top contact/top gate transistors with NH_3I-SAM. Its representative output and transfer characteristics when measured with forward and reverse scans at a scan rate of 5 V s^{-1} are shown on the right. (b) Device structure of $(4Tm)_2SnI_4$ based top contact/bottom gate and corresponding representative output and transfer characteristics. Figures reproduced with permission from: (a) ref. 61. Copyright 2016, Wiley-VCH; (b) ref. 26. Copyright 2019, American Chemical Society.

This journal is © The Royal Society of Chemistry and the Chinese Chemical Society 2020

Mater. Chem. Front., 2020, 4, 3400–3418 | 3411

4.3 Light-emitting diodes

Halide perovskites are also attractive in the realm of light-emitting diodes (LEDs). In fact, the external quantum efficiency (EQE) of devices from these materials have increased from 0.1% to over 20% since 2014 using 3D or quasi-2D perovskites.[63–68] Quasi-2D halide perovskites LEDs have shown promising results due to several desirable properties because the small grain size is beneficial for efficient radiative recombination. Thus, in a quasi-2D halide perovskites LED, not only do the bulky ligands stabilize the devices but also enhance the performance due to the nanoscale grain size induced by bulky ligand butylammonium (BA).[65] In another study, the conjugated ligand 1-naphthylmethylamine (NMA) was applied in quasi-2D halide perovskites LEDs (with $n > 3$ mixed phases), which form perovskite multiple quantum wells with an energy cascade landscape (Fig. 10a).[63] A high external quantum efficiency of over 11% was achieved. However, the light emission was believed to originate from high n number or even 3D perovskite nanoparticles embedded in the quasi-2D perovskite matrix. Despite the relatively high efficiency, the quasi-2D perovskite thin films are not stable enough and they suffer from ion-migration problems under large electrical bias.

Phase-pure 2D perovskite quantum wells with a low n number (*e.g.*, $n < 3$) are promising for highly stable LEDs because of their excellent intrinsic stability. Furthermore, the large binding energy (*i.e.*, 300–600 meV) and fast radiative recombination rate in these 2D perovskites can be beneficial for LED devices.[69] However, charge injection becomes an issue when n number is small. Novel conjugated ligands have to be carefully designed for this purposes. Increasing the conjugation usually results in shrinkage of HOMO–LUMO gap of the π-conjugated ligands. By using correct metal halide composition, type II or type I quantum well with smaller HOMO–LUMO gap could be formed.[25] In the case of type II, PL is usually quenched. In the case of type I with smaller organic HOMO–LUMO gap, the energy may transfer to organic ligands that results in EL and PL purely contributed by organic ligands.[25,70] This may introduce chances in high performance organic light emitting diodes (OLED), in which the EL originated purely from the ligands itself rather than inorganic components. This type of device, reported in 1999 is another example employing conjugated organic cations.[70] As shown in Fig. 10b, by incorporating the oligothiophene diammonium cation AEQT, the resulting (AEQT)PbCl$_4$ LED showed good carrier injection as well as good performance of 0.1 lm W^{-1} thanks to the self-assembly alternating organic dyes templated by inorganic perovskite layers. As with other OLEDs, the EL is determined by the chemistry of organic ligands. Consequently, one may tune the color by designing the desired HOMO–LUMO gap.

In order to cover a larger emission spectrum, researchers have turned their eyes onto the relatively benign Sn-based halide perovskites LEDs in the red and infrared regions.[71–76] Unfortunately, the instability that results in Sn^{4+} defects and
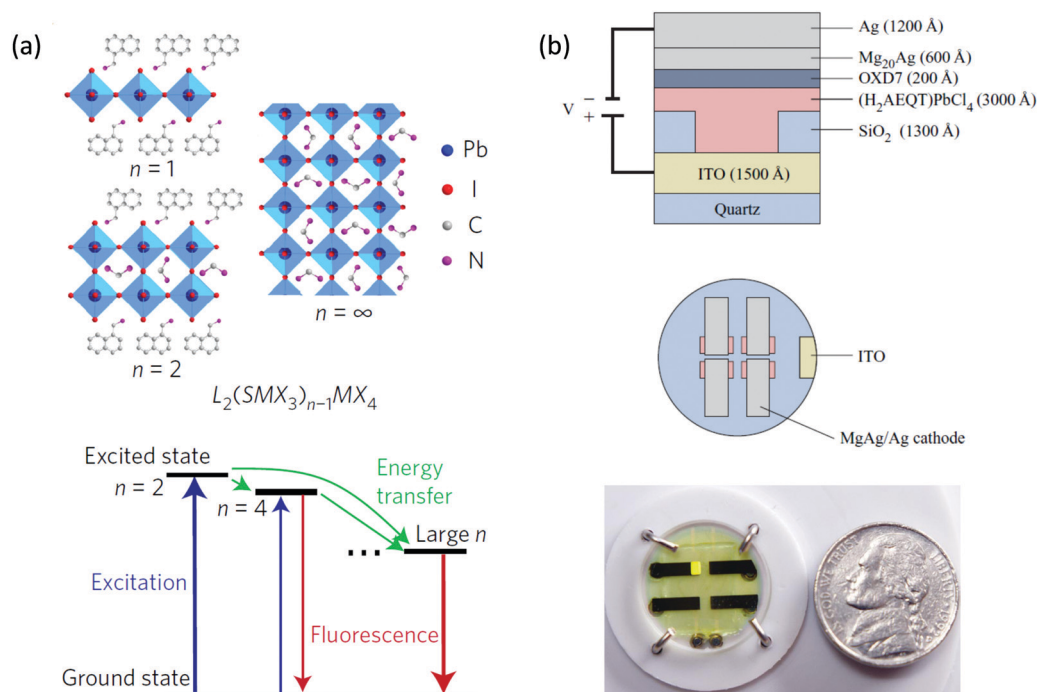
Fig. 10 (a) Schematic representation of the structures of the layered lead halide perovskites with $n = 1$, $n = 2$ and $n = \infty$ (up). Schematic of cascade energy transfer in MQWs. Excitation energy is transferred downstream from smaller-n QWs to larger-n QWs, and the emission is mainly from larger-n QWs (down). (b) Cross section of the OILED device structure and top view of the circular substrate containing four devices. Photograph of an operational OILED device based on (AEQT)PbCl$_4$ as the emitting material. Figures reproduced with permission from: (a) ref. 63. Copyright 2016, Springer Nature; (b) ref. 1. Copyright 2016, American Chemical Society.

3412 | *Mater. Chem. Front.*, 2020, **4**, 3400–3418

This journal is © The Royal Society of Chemistry and the Chinese Chemical Society 2020

low quantum yield of Sn-based halide perovskites limits the durability and performance of these devices.[71,72] Yet, the EQE of n = 1 Sn-based 2D halide perovskites LED is low ($\sim$0.1%).[73,74] Even applying the quasi-2D configuration, the EQE is still as low as 3%.[75] Recently, a Sn-based n = 1 2D halide perovskites LED based on 2-thiopheneethylamine ligand was presented. It showed a peak EQE of 0.62% with maximum luminance of 322 cd m^{-2} and pure red (638 nm) emission.[76] Compared to a PEA-based device, it shows a better charge injection and PL quantum yield. This research again highlights the importance of ligand design in terms of charge carrier motion and the promising features of aromatic moieties in organic cations. For 2D Sn-based halide perovskites, there is a chance to form the type I quantum well with more sophisticated π-conjugated ligands. In that case, EL from perovskite layers could be obtained, meanwhile, suitable HOMO–LUMO energy levels and semiconducting nature of organic layers will facilitate charge injection and transport, thus both the performance and stability are expected to be improved compared to current Sn-based counterparts.

4.4 Thermoelectric devices

Thermoelectric devices are capable of low-value thermal energy harvesting and active cooling. Lately, the application of halide perovskites in thermoelectric application has piqued the interest of the community due to the high Seebeck coefficient and low thermal conductivity associated with 3D perovskites.[77] The figure of merit for a thermoelectric material is defined as $zT = S^2\sigma/\kappa$, where S is the Seebeck coefficient, σ is the electrical conductivity and κ is the thermal conductivity.

To achieve a high zT value, one needs to increase the electrical conductivity and Seebeck coefficient of perovskite to a larger extent while decreasing the thermal conductivity. Despite many attempts to dope halide perovskites, so far, the only way to achieve high electrical conductivity of halide perovskites is by using the spontaneous p-doped Sn-based perovskites, in which Sn^{2+} is oxidized to Sn^{4+} and act as dopants.[78] Along this line of thinking, the doping and degradation process of Sn-based 2D halide perovskites can be largely slowed down by the π-conjugated ligands,[20,26] thus introducing a much larger tunability to achieve higher zT values. In addition, we expect the superlattice-like structure of 2D halide perovskites could lead to lower thermal conductivity than the already very low 3D halide perovskites. This hypothesis is based on the expected phonon scattering on the organic–inorganic interfaces,[79–81] a phenomenon that has been utilized in traditional high zT materials such as Bi$_2$Te$_3$/Sb$_2$Te$_3$ superlattices.[82] By utilizing Sn-based 2D halide perovskites and π-conjugated ligands, we expect to further improve their thermoelectric energy conversion performance.

5. Conclusions and perspectives

Organic–inorganic hybrid 2D halide perovskites represent a new class of materials that alternate chemically and electronically at

the molecular level. In turn, these materials provide new possibilities to combine desirable physical properties characteristic of both organic and inorganic components. The inorganic components offer the potential for a wide range of excellent electronic properties, substantial mechanical robustness, and thermal stability. The organic moieties, on the other hand, provide ease of processing, high fluorescence efficiency, large polarizability, plastic mechanical properties, and structural diversity. Moreover, the tunability of 2D halide perovskites allows for the incorporation of semiconducting conjugated organic building blocks, thus adding advantages over the 3D and electronically-inert spacer-containing 2D perovskites of having further enhanced environmental stability, reduced ionic migration, and easily tunable electrical properties.

Importantly, there is a wide chemical space for future materials design. For instance, a type-III band alignment design has not been achieved, nor has effective charge carrier doping been realized. New types of functional organic building blocks, such as chiral molecules, organic radical species, organothiolate linkers, and photo-switchable and polymerizable species have yet been incorporated into the inorganic lattice.[83–87] Therefore, a clear research opportunity in this field is to bring the significant advances associated with organic chemistry into the hybrid perovskite world. While care must be taken to ensure that the molecular designs of the organic components do not interrupt the structure-directing function historically associated with organic ligands in hybrid perovskite structures, the creativity and nearly-endless design space associated with organic chemistry will allow for these types of efforts to occur. Importantly, this methodology is completely in agreement with the beauty of organic design observed in many of Fred Wudl's publications, and we look forward to the community applying his pioneering approach to hybrid 2D perovskites in the near future.

This new class of 2D halide perovskites also displays tremendous potential in solar cells, FETs, LED, thermoelectric, ferroelectric and photodetector and radiation detector device applications.[88,89] Owing to the organic–inorganic hybrid nature, their heterostructures act as a great platform to explore structure property relationships and understand many fundamental chemistry and physics within these hybrid semiconductors. Notably, a series epitaxial lateral 2D perovskite heterostructures have been fabricated recently, which opens a new avenue for complex and molecularly thin superlattices, devices, and integrated circuits.[90] Colloidal lead halide perovskite quantum dots have been demonstrated for coherent single-photon emission,[91] and the recent success of double layer strategy in boosting exciton condensation temperature in transition metal dichalcogenide systems has implications for the potential of new 2D halide perovskites.[92] The layered structure of halide perovskite may also have chance of extending the exciton lifetime while still maintaining the high binding energy. Further development of exciton condensation in this new material platform may advance towards coherent optoelectronics applications and perhaps even high-temperature superconductivity. Clearly, there is tremendous of opportunities ahead. More efforts on the molecular design of the

organic cations, crystal growth strategies, photo-physics, and device engineering are required to advance this exciting field of research.

Key among these opportunities is for an increased presence with respect to theory and computational design of materials, assembly, and optoelectronic structure predictions. While high-throughput chemistry and device application have driven 2D hybrid perovskite design to date, computational efforts are quickly becoming an integral part of these efforts, and they often help explain observed experimental phenomena from a molecular approach. In the future, we anticipate that the temporal roles of experiment and computation will switch such that computation will primarily drive experiment as opposed to the current common operating paradigm. If this is to occur, the speed at which the field moves forward will be even faster than its already breakneck clip, and we welcome these types of investments.

Finally, as advanced hybrid geometries are created, an expanded set of advanced structural characterization techniques should be employed. In addition to the high-end X-ray diffraction experiments that occur at synchrotron sources currently, it is anticipated that new materials design paradigms will emerge when next-generation X-ray techniques are more oft-implemented in 2D perovskite systems. Additionally, as chemistry melds with structure and end-use application, the *in operando* evaluation of nanostructures during device application will be critical to evaluate the underlying materials and device physics associated with this emerging class of materials.

In many ways, the future of 2D hybrid perovskite materials and device is extremely bright, and we anticipate that the field will continue to grow on multiple different fronts. This emergence of new materials, devices, and opportunities will continue to bring together chemists, materials scientists, physicists, and engineers in a manner that allows for a welcoming and diverse community of researchers. In this way, we anticipate that the continued promise of the materials will continue to inspire generations of junior researchers such that continued impact will occur at both the fundamental and applied levels in a way that will eventually allow for translation of these materials into commercial products.

Conflicts of interest

The authors declare no conflicts of interests.

Acknowledgements

References

1 B. Saparov and D. B. Mitzi, Organic-inorganic perovskites: structural versatility for functional materials design, *Chem. Rev.*, 2016, **116**, 4558–4596.

2 E. Shi, Y. Gao, B. P. Finkenauer, Akriti, A. H. Coffey and L. Dou, Two-dimensional halide perovskite nanomaterials and heterostructures, *Chem. Soc. Rev.*, 2018, **47**, 6046–6072.

3 G. Lanty, K. Jemli, Y. Wei, J. Leymarie, J. Even, J.-S. Lauret and E. Deleporte, Room-temperature optical tunability and inhomogeneous broadening in 2D-layered organic-inorganic perovskite pseudobinary alloys, *J. Phys. Chem. Lett.*, 2014, **5**, 3958–3963.

4 L. T. Dou, A. B. Wong, Y. Yu, M. L. Lai, N. Kornienko, S. W. Eaton, A. Fu, C. G. Bischak, J. Ma, T. N. Ding, N. S. Ginsberg, L. W. Wang, A. P. Alivisatos and P. D. Yang, Atomically thin two-dimensional organic-inorganic hybrid perovskites, *Science*, 2015, **349**, 1518–1521.

5 M. C. Weidman, M. Seitz, S. D. Stranks and W. A. Tisdale, Highly tunable colloidal perovskite nanoplatelets through variable cation, metal, and halide composition, *ACS Nano*, 2016, **10**, 7830–7839.

6 S. Deng, E. Shi, L. Yuan, L. Jin, L. Dou and L. Huang, Long-range exciton transport and slow annihilation in two-dimensional hybrid perovskites, *Nat. Commun.*, 2020, **11**, 664.

7 L. L. Mao, C. C. Stoumpos and M. G. Kanatzidis, Two-dimensional hybrid halide perovskites: principles and promises, *J. Am. Chem. Soc.*, 2019, **141**, 1171–1190.

8 F. Zhang, H. Lu, J. Tong, J. J. Berry, M. C. Beard and K. Zhu, Advances in two-dimensional organic-inorganic hybrid perovskites, *Energy Environ. Sci.*, 2020, **13**, 1154–1186.

9 C. M. M. Soe, G. P. Nagabhushana, R. Shivaramaiah, H. Tsai, W. Nie, J.-C. Blancon, F. Melkonyan, D. H. Cao, B. Traoré, L. Pedesseau, M. Kepenekian, C. Katan, J. Even, T. J. Marks, A. Navrotsky, A. D. Mohite, C. C. Stoumpos and M. G. Kanatzidis, Structural and thermodynamic limits of layer thickness in 2D halide perovskites, *Proc. Natl. Acad. Sci. U. S. A.*, 2019, **116**, 58–66.

10 D. B. Straus and C. R. Kagan, Electrons, excitons, and phonons in two-dimensional hybrid perovskites: connecting structural, optical, and electronic properties, *J. Phys. Chem. Lett.*, 2018, **9**, 1434–1447.

11 D. B. Mitzi, Templating and structural engineering in organic-inorganic perovskites, *J. Chem. Soc., Dalton Trans.*, 2001, 1–12.

12 J. Calabrese, N. L. Jones, R. L. Harlow, N. Herron, D. L. Thorn and Y. Wang, Preparation and characterization of layered lead halide compounds, *J. Am. Chem. Soc.*, 1991, **113**, 2328–2330.

13 M. Era, K. Maeda and T. Tsutsui, Enhanced phosphorescence from naphthalene-chromophore incorporated into lead bromide-based layered perovskite having organic-inorganic superlattice structure, *Chem. Phys. Lett.*, 1998, **296**, 417–420.

14 M. Braun, W. Tuffentsammer, H. Wachtel and H. C. Wolf, Pyrene as emitting chromophore in organic-inorganic lead

3414 | *Mater. Chem. Front.*, 2020, **4**, 3400–3418

This journal is © The Royal Society of Chemistry and the Chinese Chemical Society 2020

halide-based layered perovskites with different halides, *Chem. Phys. Lett.*, 1999, **307**, 373–378.

15 W. T. M. Van Gompel, R. Herckens, K. Van Hecke, B. Ruttens, J. D'Haen, L. Lutsen and D. Vanderzande, Low-dimensional hybrid perovskites containing an organic cation with an extended conjugated system: tuning the excitonic absorption features, *ChemNanoMat*, 2019, **5**, 323–327.

16 M. Era, T. Kobayashi, K. Sakaguchi, E. Tsukamoto and Y. Oishi, Electric conduction of PbBr-based layered perovskite organic–inorganic superlattice having carbazole chromophore-linked ammonium molecule as an organic layer, *Org. Electron.*, 2013, **14**, 1313–1317.

17 H. Hu, D. Zhao, Y. Gao, X. Qiao, T. Salim, B. Chen, E. E. M. Chia, A. C. Grimsdale and Y. M. Lam, Harvesting triplet excitons in lead-halide perovskites for room-temperature phosphorescence, *Chem. Mater.*, 2019, **31**, 2597–2602.

18 K. Jemli, P. Audebert, L. Galmiche, G. Le Trippe-Allard, D. Garrot, J. S. Lauret and E. Deeporte, Two-dimensional perovskite activation with an organic luminophore, *ACS Appl. Mater. Interfaces*, 2015, **7**, 21763–21769.

19 K. Z. Du, Q. Tu, X. Zhang, Q. W. Han, J. Liu, S. Zauscher and D. B. Mitzi, Two-dimensional lead(II) halide-based hybrid perovskites templated by acene alkylamines: crystal structures, optical properties, and piezoelectricity, *Inorg. Chem.*, 2017, **56**, 9291–9302.

20 I. H. Park, L. Chu, K. Leng, Y. F. Choy, W. Liu, I. Abdelwahab, Z. Zhu, Z. Ma, W. Chen, Q. H. Xu, G. Eda and K. P. Loh, Highly stable two-dimensional tin(II) iodide hybrid organic-inorganic perovskite based on stilbene derivative, *Adv. Funct. Mater.*, 2019, **29**, 1904810.

21 J. V. Passarelli, D. J. Fairfield, N. A. Sather, M. P. Hendricks, H. Sai, C. L. Stern and S. I. Stupp, Enhanced out-of-plane conductivity and photovoltaic performance in $n = 1$ layered perovskites through organic cation design, *J. Am. Chem. Soc.*, 2018, **140**, 7313–7323.

22 D. Cortecchia, C. Soci, M. Cametti, A. Petrozza and J. Marti-Rujas, Crystal engineering of a two-dimensional lead-free perovskite with functional organic cations by second-sphere coordination, *ChemPlusChem*, 2017, **82**, 681–685.

23 D. B. Mitzi, K. Chondroudis and C. R. Kagan, Design, structure, and optical properties of organic-inorganic perovskites containing an oligothiophene chromophore, *Inorg. Chem.*, 1999, **38**, 6246–6256.

24 X. H. Zhu, N. Mercier, P. Frere, P. Blanchard, J. Roncali, M. Allain, C. Pasquier and A. Riou, Effect of mono- versus di-ammonium cation of 2,2′-bithiophene derivatives on the structure of organic-inorganic hybrid materials based on iodo metallates, *Inorg. Chem.*, 2003, **42**, 5330–5339.

25 Y. Gao, E. Z. Shi, S. B. Deng, S. B. Shiring, J. M. Snaider, C. Liang, B. Yuan, R. Y. Song, S. M. Janke, A. Liebman-Pelaez, P. Yoo, M. Zeller, B. W. Boudouris, P. L. Liao, C. H. Zhu, V. Blum, Y. Yu, B. M. Savoie, L. B. Huang and L. T. Dou, Molecular engineering of organic-inorganic hybrid perovskites quantum wells, *Nat. Chem.*, 2019, **11**, 1151–1157.

26 Y. Gao, Z. T. Wei, P. Yoo, E. Z. Shi, M. Zeller, C. H. Zhu, P. L. Liao and L. T. Dou, Highly stable lead-free perovskite field-effect transistors incorporating linear π-conjugated organic ligands, *J. Am. Chem. Soc.*, 2019, **141**, 15577–15585.

27 Y. Takeoka, K. Asai, M. Rikukawa and K. Sanui, Incorporation of conjugated polydiacetylene systems into organic-inorganic quantum-well structures, *Chem. Commun.*, 2001, 2592–2593.

28 C. Ortiz-Cervantes, P. I. Román-Román, J. Vazquez-Chavez, M. Hernández-Rodríguez and D. Solis-Ibarra, Thousand-fold conductivity increase in 2D perovskites by polydiacetylene incorporation and doping, *Angew. Chem., Int. Ed.*, 2018, **57**, 13882–13886.

29 M. Era, S. Yoneda, T. Sano and M. Noto, Preparation of amphiphilic poly(thiophene)s and their application for the construction of organic-inorganic superlattices, *Thin Solid Films*, 2003, **438–439**, 322–325.

30 F. H. Isikgor, C. D. Reddy, M. S. Li, H. Coskun, B. C. Li, Y. W. Zhang, S. J. Pennycook and J. Y. Ouyang, Self-assembled atomically thin hybrid conjugated polymer perovskites with two-dimensional structure, *J. Mater. Chem. C*, 2018, **6**, 8405–8410.

31 H. P. Xu, J. Z. Sun, A. J. Qin, J. L. Hua, Z. Li, Y. Q. Dong, H. Xu, W. Z. Yuan, Y. G. Ma, M. Wang and B. Z. Tang, Functional perovskite hybrid of polyacetylene ammonium and lead bromide: synthesis, light emission, and fluorescence imagining, *J. Phys. Chem. B*, 2006, **110**, 21701–21709.

32 W. A. Dunlap-Shohl, E. T. Barraza, A. Barrette, S. Dovletgeldi, G. Findik, D. J. Dirkes, C. Liu, M. K. Jana, V. Blum, W. You, K. Gundogdu, A. D. Stiff-Roberts and D. B. Mitzi, Tunable internal quantum well alignment in rationally designed oligomer-based perovskite films deposited by resonant infrared matrix-assisted pulsed laser evaporation, *Mater. Horiz.*, 2019, **6**, 1707–1716.

33 G. C. Papavassiliou, G. A. Mousdis, G. Pagona, N. Karousis and M.-S. Vidali, Room temperature enhanced blue-green, yellow-orange and red phosphorescence from some compounds of the type $(CH_3NH_3)_{n-1}$(1-naphthylmethyl ammonium)$_2$Pb$_n$(Cl$_x$Br$_{1-x}$)$_{3n+1}$ (with $n = 1$, 2 and $0 \leq x \leq 1$) and related observations from similar compounds, *J. Lumin.*, 2014, **149**, 287–291.

34 C. Liu, W. Huhn, K.-Z. Du, A. Vazquez-Mayagoitia, D. Dirkes, W. You, Y. Kanai, D. B. Mitzi and V. Blum, Tunable semiconductors: control over carrier states and excitations in layered hybrid organic-inorganic perovskites, *Phys. Rev. Lett.*, 2018, **121**, 146401.

35 Z. Y. Wang, A. M. Ganose, C. M. Niu and D. O. Scanlon, Two-dimensional eclipsed arrangement hybrid perovskites for tunable energy level alignments and photovoltaics, *J. Mater. Chem. C*, 2019, **7**, 5139–5147.

36 S. Deng, J. M. Snaider, Y. Gao, E. Shi, L. Jin, R. D. Schaller, L. Dou and L. Huang, Long-lived charge separation in two-dimensional ligand-perovskite heterostructures, *J. Chem. Phys.*, 2020, **152**, 044711.

37 K. Ema, M. Inomata, Y. Kato, H. Kunugita and M. Era, Nearly perfect triplet-triplet energy transfer from Wannier

This journal is © The Royal Society of Chemistry and the Chinese Chemical Society 2020

Mater. Chem. Front., 2020, **4**, 3400–3418 | **3415**

excitons to naphthalene in organic-inorganic hybrid quantum-well materials, *Phys. Rev. Lett.*, 2008, **100**, 257401.

38 M. Braun, W. Tuffentsammer, H. Wachtel and H. C. Wolf, Tailoring of energy levels in lead chloride based layered perovskites and energy transfer between the organic and inorganic planes, *Chem. Phys. Lett.*, 1999, **303**, 157–164.

39 S. Yang, D. Wu, W. Gong, Q. Huang, H. Zhen, Q. Ling and Z. Lin, Highly efficient room-temperature phosphorescence and afterglow luminescence from common organic fluorophores in 2D hybrid perovskites, *Chem. Sci.*, 2018, **9**, 8975–8981.

40 D. B. Mitzi, Organic-inorganic perovskites containing trivalent metal halide layers: the templating influence of the organic cation layer, *Inorg. Chem.*, 2000, **39**, 6107–6113.

41 H. A. Evans, A. J. Lehner, J. G. Labram, D. H. Fabini, O. Barreda, S. R. Smock, G. Wu, M. L. Chabinyc, R. Seshadri and F. Wudl, (TTF)Pb₂I₅: a radical cation-stabilized hybrid lead iodide with synergistic optoelectronic signatures, *Chem. Mater.*, 2016, **28**, 3607–3611.

42 M. K. Jana, S. M. Janke, D. J. Dirkes, S. Dovletgeldi, C. Liu, X. X. Qin, K. Gundogdu, W. You, V. Blum and D. B. Mitzi, Direct-bandgap 2D silver-bismuth iodide double perovskite: the structure-directing influence of an oligothiophene spacer cation, *J. Am. Chem. Soc.*, 2019, **141**, 7955–7964.

43 N. R. Venkatesan, A. Mandi, B. Barraza, G. Wu, M. L. Chabinyc and R. Seshadri, Enhanced yield-mobility products in hybrid halide Ruddlesden-Popper compounds with aromatic ammonium spacers, *Dalton Trans.*, 2019, **48**, 14019–14026.

44 J. Ahn, S. Ma, J. Y. Kim, J. Kyhm, W. Yang, J. A. Lim, N. A. Kotov and J. Moon, Chiral 2D organic inorganic hybrid perovskite with circular dichroism tunable over wide wavelength range, *J. Am. Chem. Soc.*, 2020, **142**, 4206–4212.

45 W. T. M. Van Gompel, R. Herckens, K. Van Hecke, B. Ruttens, J. D'Haen, L. Lutsen and D. Vanderzande, Towards 2D layered hybrid perovskites with enhanced functionality: introducing charge-transfer complexes via self-assembly, *Chem. Commun.*, 2019, **55**, 2481–2484.

46 H. Tsai, W. Nie, J. C. Blancon, C. C. Stoumpos, R. Asadpour, B. Harutyunyan, A. J. Neukirch, R. Verduzco, J. J. Crochet, S. Tretiak, L. Pedesseau, J. Even, M. A. Alam, G. Gupta, J. Lou, P. M. Ajayan, M. J. Bedzyk and M. G. Kanatzidis, High-efficiency two-dimensional Ruddlesden-Popper perovskite solar cells, *Nature*, 2016, **536**, 312–316.

47 L. Yan, J. Hu, Z. Guo, H. Chen, M. F. Toney, A. M. Moran and W. You, General post-annealing method enables high-efficiency two-dimensional perovskite solar cells, *ACS Appl. Mater. Interfaces*, 2018, **10**, 33187–33197.

48 L. N. Quan, M. Yuan, R. Comin, O. Voznyy, E. M. Beauregard, S. Hoogland, A. Buin, A. R. Kirmani, K. Zhao, A. Amassian, D. H. Kim and E. H. Sargent, Ligand-stabilized reduced-dimensionality perovskites, *J. Am. Chem. Soc.*, 2016, **138**, 2649–2655.

49 C. C. Stoumpos, C. M. M. Soe, H. Tsai, W. Nie, J.-C. Blancon, D. H. Cao, F. Liu, B. Traore, C. Katan, J. Even, A. D. Mohite and M. G. Kanatzidis, High members of the 2D Ruddlesden-Popper halide perovskites: synthesis, optical properties, and

50 A. H. Proppe, R. Quintero-Bermudez, H. Tan, O. Voznyy, S. O. Kelley and E. H. Sargent, Synthetic control over quantum well width distribution and carrier migration in low-dimensional perovskite photovoltaics, *J. Am. Chem. Soc.*, 2018, **140**, 2890–2896.

51 C. M. M. Soe, W. Nie, C. C. Stoumpos, H. Tsai, J.-C. Blancon, F. Liu, J. Even, T. J. Marks, A. D. Mohite and M. G. Kanatzidis, Understanding film formation morphology and orientation in high member 2D Ruddlesden-Popper perovskites for high-efficiency solar cells, *Adv. Energy Mater.*, 2018, **8**, 1700979.

52 Z. Wang, Q. Lin, F. P. Chmiel, N. Sakai, L. M. Herz and H. J. Snaith, Efficient ambient-air-stable solar cells with 2D-3D heterostructured butylammonium-caesium-formamidinium lead halide perovskites, *Nat. Energy*, 2017, **2**, 17135.

53 H. Dong, J. Xi, L. Zuo, J. Li, Y. Yang, D. Wang, Y. Yu, L. Ma, C. Ran, W. Gao, B. Jiao, J. Xu, T. Lei, F. Wei, F. Yuan, L. Zhang, Y. Shi, X. Hou and Z. Wu, Conjugated molecules "bridge": functional ligand toward highly efficient and long-term stable perovskite solar cell, *Adv. Funct. Mater.*, 2019, **29**, 1808119.

54 F. Wei, B. Jiao, H. Dong, J. Xu, T. Lei, J. Zhang, Y. Yu, L. Ma, D. Wang, J. Chen, X. Hou and Z. Wu, Bifunctional π-conjugated ligand assisted stable and efficient perovskite solar cell fabrication via interfacial stitching, *J. Mater. Chem. A*, 2019, **7**, 16533–16540.

55 I. Zimmermann, S. Aghazada and M. K. Nazeeruddin, Lead and HTM free stable two-dimensional tin perovskites with suitable band gap for solar cell applications, *Angew. Chem., Int. Ed.*, 2019, **58**, 1072–1076.

56 D. Li, H. C. Cheng, Y. Wang, Z. Zhao, G. Wang, H. Wu, Q. He, Y. Huang and X. Duan, The effect of thermal annealing on charge transport in organolead halide perovskite microplate field-effect transistors, *Adv. Mater.*, 2017, **29**, 1601959.

57 Y. H. Lin, P. Pattanasattayavong and T. D. Anthopoulos, Metal-halide perovskite transistors for printed electronics: challenges and opportunities, *Adv. Mater.*, 2017, **29**, 1702838.

58 S. P. Senanayak, B. Yang, T. H. Thomas, N. Giesbrecht, W. Huang, E. Gann, B. Nair, K. Goedel, S. Guha, X. Moya, C. R. McNeill, P. Docampo, A. Sadhanala, R. H. Friend and H. Sirringhaus, Understanding charge transport in lead iodide perovskite thin-film field-effect transistors, *Sci. Adv.*, 2017, **3**, e1601935.

59 X. Liu, D. Yu, X. Song and H. Zeng, Metal halide perovskites: synthesis, ion migration, and application in field-effect transistors, *Small*, 2018, **14**, e1801460.

60 C. R. Kagan, D. B. Mitzi and C. D. Dimitrakopoulos, Organic-inorganic hybrid materials as semiconducting channels in thin-film field-effect transistors, *Science*, 1999, **286**, 945–947.

61 T. Matsushima, S. Hwang, A. S. Sandanayaka, C. Qin, S. Terakawa, T. Fujihara, M. Yahiro and C. Adachi, Solution-processed organic-inorganic perovskite field-effect transistors with high hole mobilities, *Adv. Mater.*, 2016, **28**, 10275–10281.

solar cells of (CH₃(CH₂)₃NH₃)₂(CH₃NH₃)₄Pb₅I₁₆, *Chem*, 2017, **2**, 427–440.

62 T. Matsushima, S. Hwang, S. Terakawa, T. Fujihara, A. S. D. Sandanayaka, C. Qin and C. Adachi, Intrinsic carrier transport properties of solution-processed organic-inorganic perovskite films, *Appl. Phys. Express*, 2017, **10**, 024103.

63 N. Wang, L. Cheng, R. Ge, S. Zhang, Y. Miao, W. Zou, C. Yi, Y. Sun, Y. Cao, R. Yang, Y. Wei, Q. Guo, Y. Ke, M. Yu, Y. Jin, Y. Liu, Q. Ding, D. Di, L. Yang, G. Xing, H. Tian, C. Jin, F. Gao, R. H. Friend, J. Wang and W. Huang, Perovskite light-emitting diodes based on solution-processed self-organized multiple quantum wells, *Nat. Photonics*, 2016, **10**, 699–704.

64 M. Yuan, L. N. Quan, R. Comin, G. Walters, R. Sabatini, O. Voznyy, S. Hoogland, Y. Zhao, E. M. Beauregard, P. Kanjanaboos, Z. Lu, D. H. Kim and E. H. Sargent, Perovskite energy funnels for efficient light-emitting diodes, *Nat. Nanotechnol.*, 2016, **11**, 872–877.

65 Z. Xiao, R. A. Kerner, L. Zhao, N. L. Tran, K. M. Lee, T.-W. Koh, G. D. Scholes and B. P. Rand, Efficient perovskite light-emitting diodes featuring nanometre-sized crystallites, *Nat. Photonics*, 2017, **11**, 108–115.

66 Y. Cao, N. Wang, H. Tian, J. Guo, Y. Wei, H. Chen, Y. Miao, W. Zou, K. Pan, Y. He, H. Cao, Y. Ke, M. Xu, Y. Wang, M. Yang, K. Du, Z. Fu, D. Kong, D. Dai, Y. Jin, G. Li, H. Li, Q. Peng, J. Wang and W. Huang, Perovskite light-emitting diodes based on spontaneously formed submicrometre-scale structures, *Nature*, 2018, **562**, 249–253.

67 K. Lin, J. Xing, L. N. Quan, F. P. G. de Arquer, X. Gong, J. Lu, L. Xie, W. Zhao, D. Zhang, C. Yan, W. Li, X. Liu, Y. Lu, J. Kirman, E. H. Sargent, Q. Xiong and Z. Wei, Perovskite light-emitting diodes with external quantum efficiency exceeding 20 per cent, *Nature*, 2018, **562**, 245–248.

68 W. Xu, Q. Hu, S. Bai, C. Bao, Y. Miao, Z. Yuan, T. Borzda, A. J. Barker, E. Tyukalova, Z. Hu, M. Kawecki, H. Wang, Z. Yan, X. Liu, X. Shi, K. Uvdal, M. Fahlman, W. Zhang, M. Duchamp, J.-M. Liu, A. Petrozza, J. Wang, L.-M. Liu, W. Huang and F. Gao, Rational molecular passivation for high-performance perovskite light-emitting diodes, *Nat. Photonics*, 2019, **13**, 418–424.

69 A. Molina-Sánchez, Excitonic states in semiconducting two-dimensional perovskites, *ACS Appl. Energy Mater.*, 2018, **1**, 6361–6367.

70 K. Chondroudis and D. B. Mitzi, Electroluminescence from an organic-inorganic perovskite incorporating a quaterthiophene dye within lead halide perovskite layers, *Chem. Mater.*, 1999, **11**, 3028–3030.

71 W. L. Hong, Y. C. Huang, C. Y. Chang, Z. C. Zhang, H. R. Tsai, N. Y. Chang and Y. C. Chao, Efficient low-temperature solution-processed lead-free perovskite infrared light-emitting diodes, *Adv. Mater.*, 2016, **28**, 8029–8036.

72 M. L. Lai, T. Y. Tay, A. Sadhanala, S. E. Dutton, G. Li, R. H. Friend and Z. K. Tan, Tunable near-infrared luminescence in tin halide perovskite devices, *J. Phys. Chem. Lett.*, 2016, **7**, 2653–2658.

73 L. Lanzetta, J. M. Marin-Beloqui, I. Sanchez-Molina, D. Ding and S. A. Haque, Two-dimensional organic tin halide perovskites with tunable visible emission and their use in light-emitting devices, *ACS Energy Lett.*, 2017, **2**, 1662–1668.

74 X. Zhang, C. Wang, Y. Zhang, X. Zhang, S. Wang, M. Lu, H. Cui, S. V. Kershaw, W. W. Yu and A. L. Rogach, Bright orange electroluminescence from lead-free two-dimensional perovskites, *ACS Energy Lett.*, 2018, **4**, 242–248.

75 Y. Wang, R. Zou, J. Chang, Z. Fu, Y. Cao, L. Zhang, Y. Wei, D. Kong, W. Zou, K. Wen, N. Fan, N. Wang, W. Huang and J. Wang, Tin-based multiple quantum well perovskites for light-emitting diodes with improved stability, *J. Phys. Chem. Lett.*, 2019, **10**, 453–459.

76 Z. Wang, F. Wang, B. Zhao, S. Qu, T. Hayat, A. Alsaedi, L. Sui, K. Yuan, J. Zhang, Z. Wei and Z. Tan, Efficient two-dimensional tin halide perovskite light-emitting diodes via a spacer cation substitution strategy, *J. Phys. Chem. Lett.*, 2020, **11**, 1120–1127.

77 A. Filippetti, C. Caddeo, P. Delugas and A. Mattoni, Appealing perspectives of hybrid lead-iodide perovskites as thermoelectric materials, *J. Phys. Chem. C*, 2016, **120**, 28472–28479.

78 T. Liu, X. Zhao, J. Li, Z. Liu, F. Liscio, S. Milita, B. C. Schroeder and O. Fenwick, Enhanced control of self-doping in halide perovskites for improved thermoelectric performance, *Nat. Commun.*, 2019, **10**, 5750.

79 L. D. Hicks and M. S. Dresselhaus, Effect of quantum-well structures on the thermoelectric figure of merit, *Phys. Rev. B: Condens. Matter Mater. Phys.*, 1993, **47**, 12727–12731.

80 M. S. Dresselhaus, G. Chen, M. Y. Tang, R. G. Yang, H. Lee, D. Z. Wang, Z. F. Ren, J. P. Fleurial and P. Gogna, New directions for low-dimensional thermoelectric materials, *Adv. Mater.*, 2007, **19**, 1043–1053.

81 K. Kothari and M. Maldovan, Phonon surface scattering and thermal energy distribution in superlattices, *Sci. Rep.*, 2017, **7**, 5625.

82 R. Venkatasubramanian, E. Siivola, T. Colpitts and B. O'Quinn, Thin-film thermoelectric devices with high room-temperature figures of merit, *Nature*, 2001, **413**, 597–602.

83 M. Era, Y. Shironita and K. Soda, Lead bromide-based layered perovskite Langmuir–Blodgett films having π-conjugated molecules as organic layer prepared by using squeezed out technique, *Jpn. J. Appl. Phys.*, 2018, **57**, 03EG07.

84 Y. Joo, V. Agarkar, S. H. Sung, B. M. Savoie and B. W. Boudouris, A nonconjugated radical polymer glass with high electrical conductivity, *Science*, 2018, **359**, 1391–1395.

85 X. Hu, H. Chen, L. Zhao, M.-S. Miao, X. Zheng and Y. Zheng, Nitrogen-coupled blatter diradicals: the fused *versus* unfused bridges, *J. Mater. Chem. C*, 2019, **7**, 10460–10464.

86 J. Ma, C. Fang, C. Chen, L. Jin, J. Wang, S. Wang, J. Tang and D. Li, Chiral 2D perovskites with a high degree of circularly polarized photoluminescence, *ACS Nano*, 2019, **13**, 3659–3665.

87 A. H. Coffey, P. Yoo, D. H. Kim, Akriti, M. Zeller, S. Avetian, L. Huang, P. Liao and L. Dou, Structural tunability and diversity of two-dimensional lead halide benzenethiolate, *Chem. – Eur. J.*, 2020, **26**, 6599–6607.

88 Akriti, E. Shi and L. Dou, A leap towards high-performance 2D perovskite photodetectors, *Trends Chem.*, 2019, **1**, 365–367.

89 Y. Liu, H. Ye, Y. Zhang, K. Zhao, Z. Yang, Y. Yuan, H. Wu, G. Zhao, Z. Yang, J. Tang, Z. Xu and S. Liu, Surface-tension-controlled crystallization for high-quality 2D perovskite single crystals for ultrahigh photodetection, *Matter*, 2019, **1**, 465–480.

90 E. Shi, B. Yuan, S. B. Shiring, Y. Gao, Akriti, Y. Guo, C. Su, M. Lai, P. Yang, J. Kong, B. M. Savoie, Y. Yu and L. Dou, Two-dimensional halide perovskite lateral epitaxial hetero-structures, *Nature*, 2020, **580**, 614–620.

91 H. Utzat, W. Sun, A. E. K. Kaplan, F. Krieg, M. Ginterseder, B. Spokoyny, N. D. Klein, K. E. Shulenberger, C. F. Perkinson, M. V. Kovalenko and M. G. Bawendi, Coherent single-photon emission from colloidal lead halide perovskite quantum dots, *Science*, 2019, **363**, 1068–1072.

92 Z. Wang, D. A. Rhodes, K. Watanabe, T. Taniguchi, J. C. Hone, J. Shan and K. F. Mak, Evidence of high-temperature exciton condensation in two-dimensional atomic double layers, *Nature*, 2019, **574**, 76–80.